Siliciclastic Back-Barrier Tidal Flats

10

Burghard W. Flemming

Abstract

Back-barrier tidal flats occur along micro- to mesotidal coasts landward of barrier islands and in the shelter of coastal sand spits and bars. Tidal flats are generally flood dominated, the grain size progressively decreasing shoreward. The sediment can be divided into sand, slightly muddy sand, muddy sand, sandy mud, slightly sandy mud, and mud. The mud fraction consists of non-cohesive sortable silt and cohesive flocs and aggregates. Important physical and biological surface structures include wave- and current-generated ripples, ladderback ripples, washed out ripples and other late-stage emergence runoff features, shell pavements, fluid mud sheets, tool marks, crawling, feeding and resting traces of intertidal organisms, as well as the feeding traces and tracks of birds. Internal sedimentary structures range from rare dune cross-bedding to ubiquitous ripple cross-bedding in sand, through flaser, wavy and lenticular bedding in mixed sediment, and homogenous or laminated mud toward the high-water line. Bioturbation may be intense, but the preservation potential depends on the frequency and depth of reworking. The transition from land to sea is typically marked by laminated versicolored microbial mats. The interaction between sea-level rise and sediment supply defines the sediment budget and hence the stratigraphy. Prograding, aggrading or transgressive systems are easily distinguished by their stratigraphic architecture.

10.1 Introduction

This chapter deals with non-vegetated or bare (inter) tidal flat depositional systems that occur in the shelter of coastal barriers and which are predominantly composed of siliciclastic sediments (sand and mud) of terrigenous origin. In these systems, bioclastic material derived from shell-bearing organisms, especially molluscs, forms an overall subordinate sedimentary component, although it may locally be enriched in the form of shell beds and channel lag deposits. Back-barrier tidal flats commonly occur along micro- to mesotidal coasts (tidal ranges of ~0.3–3.5 m) in the rear of barrier islands, and in the shelter of coastal sand spits. Specifically excluded are carbonate tidal deposits (Pratt et al. 1992), intertidal sand bodies occurring along lower courses of many barred estuaries (Dalrymple et al. 1992), episodically flooded back-barrier wind flats (Miller 1975; Schneider 1975), tidal lagoons without substantial intertidal flats (Ashley 1988;

B.W. Flemming (✉)
Senckenberg Institute, Suedstrand 40, 26382 Wihelmshaven, Germany
e-mail: bflemming@senckenberg.de

R.A. Davis, Jr. and R.W. Dalrymple (eds.), *Principles of Tidal Sedimentology*,
DOI 10.1007/978-94-007-0123-6_10, © Springer Science+Business Media B.V. 2012

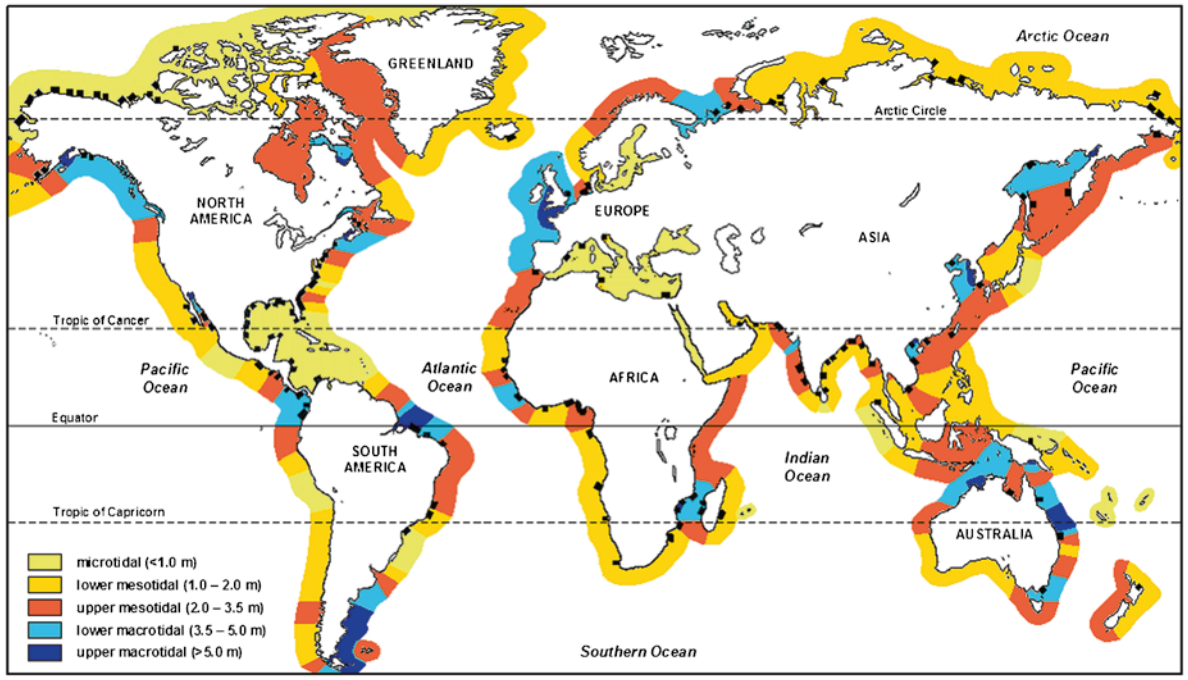

Fig. 10.1 Global distribution of coastal barriers backed by tidal flats and/or lagoons (Amended after Pilkey 2003) in relation to tidal regime (Modified after Flemming 2005)

Boothroyd et al. 1985), and extensively vegetated intertidal flats (Pestrong 1972; Frey and Basan 1985), in particular comprising cordgrass (*Spartina sp.*) marshes or mangrove forests. The stratigraphy and facies successions of these latter systems are distinctly different from those of typical non-vegetated, back-barrier tidal flat systems (Kraft et al. 1979), of which the Ria Formosa along the Algarve coast of Portugal (Pilkey et al. 1989) is a partial and the Wadden Sea lining the coasts of The Netherlands, Germany and Denmark a prime example (Bartholdy and Pejrup 1994; Flemming and Davis 1994; Oost and de Boer 1994).

A comprehensive global inventory and classification of barred tidal flat systems is currently still lacking, but as most are associated with coastal barrier systems, the amended global map of the latter (Fig. 10.1) provides a reasonable, if incomplete, picture of their geographic distribution. From Fig. 10.1 it is clearly evident that barrier islands and other types of barred coasts are not evenly distributed along the shores of the world, the vast majority being associated with low-lying coastal plains (~72%) and river deltas (~28%) (Pilkey 2003). In the context of global tectonics, 49% of barrier islands are located along trailing-edge coasts, 24% along collision coasts, and 27% along marginal sea coasts (Glaeser 1978). Furthermore, of those located along trailing-edge coasts, 75% occur along amero-trailing-edge, 19% along afro-trailing-edge, and only 6% along neo-trailing-edge coasts. These barrier systems occupy 12–13% of the world's shoreline, the greater part being represented by the lagoonal type where fringing intertidal flats are heavily vegetated by cordgrass (from subtropical to boreal climates) or mangrove forests (from subtropical to tropical climates), bare intertidal flats being reduced to narrow belts along tidal channels.

The unique nature of bare tidal flat landscapes had already been recognized by the Roman geographer Pliny the Elder (ca. AD 45) who, after having personally visited the Wadden Sea coast, describes it in his epochal geographic compendium "Historia Naturalis" as an immeasurable expanse of land inundated twice a day by sea water and of which it was uncertain whether it formed part of the land or the sea. Proper tidal flat research, however, merely dates back to the first part of

the twentieth century (Kindle 1917), especially when, in 1928, Rudolf Richter founded the Senckenberg Research Station for Marine Geology and Palaeontology in Wilhelmshaven on the North Sea coast of Germany. It was the first institution worldwide specifically dedicated to tidal flat research (Ginsburg 1975). Earlier studies either focused on regional physiographic descriptions (Arends 1833), coastal barrier formation (de Bèaumont 1845), or shore processes in general (Johnson 1919). Selections of historical benchmark papers on barrier islands and tidal flats can be found in Schwartz (1973) and Klein (1976). Recent summaries of the main characteristics of tidal flats and tidal environments can be found in Flemming (2003a, b, 2005).

10.2 Hydrological Constraints

Barrier island systems, and hence back-barrier tidal flats, are typically restricted to tidal ranges of up to about 3.5 m (Hayes 1979). Above this limit, the tidal prism or water masses moving toward and away from the coast during each tidal cycle are generally so large that there is literally no room left for barrier islands to exist, wave action being unable to counteract the strong tidal currents. The tidal prism is a function of tidal range, basin surface area and filling efficiency, the latter depending on the inlet cross-section (Van Veen 1950). As a consequence, barrier islands progressively decrease in size the larger the tidal prism gets with increasing tidal range (Oost and de Boer 1994; Davis and Flemming 1995) before degenerating into scattered ephemeral sand bank islands when a certain limit is exceeded (Reineck 1987). Because of this, Hayes (1979) proposed a new tidal classification in which five subdivisions are distinguished (<1 m: microtidal; 1–2 m: lower mesotidal; 2–3.5 m: upper mesotidal; 3.5–5.0 m: lower macrotidal; >5.0 m: upper macrotidal) (Fig. 10.2). It represents a refinement of the more commonly used classification of Davies (1964) that only distinguishes three categories (<2 m: microtidal; 2–4 m: mesotidal; >4 m: macrotidal). The geographic distribution of tidal ranges according to the more detailed classification of Hayes (1979) has been included in Fig. 10.1 and can also be found in Flemming (2005). In addition to being morphogenetically more meaningful, it also provides a much better spatial resolution of tidal regimes around the world than the older one.

As shown by Davis and Hayes (1984), a second important hydrodynamic factor limiting barrier stability

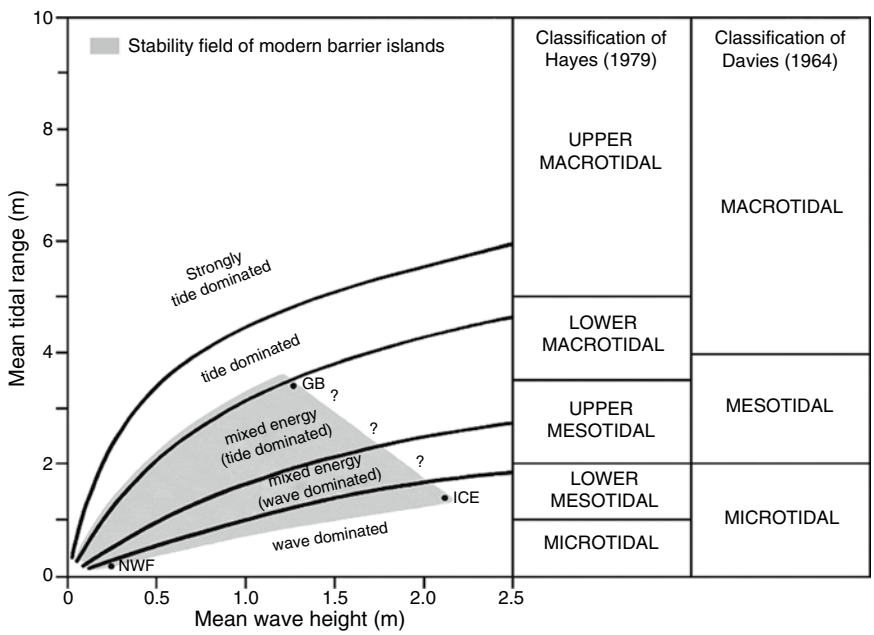

Fig. 10.2 Barrier-island stability as a function of wave climate and tidal range relative to the classification schemes of Davies (1964) and Hayes (1979)

is the wave climate. Thus, sandy barriers are today restricted to coasts exposed to mean wave heights of less than about 2.2 m (Hayes 1979). In terms of wave climate and tidal range, the stability field of modern sand barriers essentially occupies the mixed wave- and tide-dominated energy regimes (Fig. 10.2). In this interacting, relative energy constellation the Gulf coast of north-west Florida (NWF), for example, represents a low wave/low tidal energy endmember, the German Bight (GB) an intermediate wave/high tidal energy endmember, and the barrier coast of south-eastern Iceland (ICE) a high wave/intermediate tidal energy endmember. To date it is not clear whether the boundaries of this stability field, especially the one between the GB and ICE endmembers, are definitive or purely fortuitous, the occurrence of gravelly barriers in macrotidal environments suggesting that grain size may play an important additional role (Jennings and Coventry 1973; Hayes 1994).

In contrast to the processes along the open coast, the tidal basins on the landward side of barriers are predominantly controlled by tidal energy fluxes, although wave action is an important secondary factor, as emphasised by the ubiquitous occurrence of wave-generated sedimentary structures. The high correlations between physical parameters such as the surface area of a tidal basin, tidal prism, tidal discharge, inlet width, inlet cross-section, inlet depth, channel depth, and ebb-delta area and volume document the overriding control by the tides (Walther 1972; Jarrett 1976; Walton and Adams 1976; Hume and Herdendorf 1992; Flemming and Davis 1994; van Dongeren and de Vriend 1994; Biegel and Hoekstra 1995; van der Spek 1995; Williams et al. 2002). With respect to back-barrier tidal flats, important hydrological factors are the time/distance velocity asymmetries between flood and ebb currents, tidal flats being generally flood dominated, whereas deeper channels are ebb dominated (Groen 1967; Boon and Byrne 1981; Aubrey and Speer 1985; Speer and Aubrey 1985; Dronkers 1986; Ridderinkhof 1988; Friedrichs and Aubrey 1988; Friedrichs et al. 1992; Stanev et al. 2007). This has two important implications. First, the residual current over intertidal shoals (tide-induced drift) results in a net shoreward transport of suspended sediment, a process that may be enhanced or retarded by wind stress and wave action. An additional factor may be the development of horizontal density gradients over tidal flats, as recently proposed by Burchard et al. (2008). Suspended particulate matter (SPM) eventually settles out in places where the settling velocity exceeds the erosion velocity. This process acts in conjunction with the settling lag/scour lag mechanism (van Straaten and Kuenen 1957; Postma 1961) which is responsible for an overall stepwise net displacement of resuspended particles in the direction of the flood current. By this mechanism suspended particles settle out at high water slack tide before being resuspended in the course of the subsequent ebbing tide. As the particles require higher velocities to be resuspended than to settle out, the time-velocity asymmetry between the ebb and flood phase produces a net landward transport. This mechanism proceeds until a balance between settling velocity and erosion velocity is reached. The resulting shoreward decrease in grain size is one of the main consequences and hence a fundamental diagnostic criteria for intertidal deposits (e.g., van Straaten and Kuenen 1957, 1958; Nyandwi and Flemming 1995; Chang and Flemming 2006).

Both mechanisms outlined above may be strongly enhanced by seasonal changes in water temperature which, at higher latitudes, may differ by >20°C. The higher kinematic viscosities of the seawater in winter result in lower settling velocities of equivalent particles, i.e. the same particles behave as coarser sediment in summer and finer sediment in winter (Anderson 1983; Krögel and Flemming 1998; Chang et al. 2006a). That this effect is significant is demonstrated by the fact that, for example in the Wadden Sea (>55°N), particles with equivalent settling velocities in winter (T <5°C) and summer (T >20°C) are spatially separated by as much as 3 km (Fig. 10.3).

A second implication is that the channel systems of back-barrier tidal basins are not landward-facing flooding systems, but rather seaward-facing drainage systems analogous to terrestrial drainage networks (Flemming and Davis 1994). However, as the flow is bidirectional, there are some morphological modifications associated with flow separation between the dominant ebb and the subordinate flood current (Jakobsen 1962; van Straaten 1964). This flow separation is modulated by the Coriolis effect, which deflects the flow to the right in the Northern and to the left in the Southern Hemisphere. As a consequence, tidal channels are frequently split longitudinally into ebb- and flood-dominated sections that can, for example, be identified by the corresponding orientation of larger bedforms.

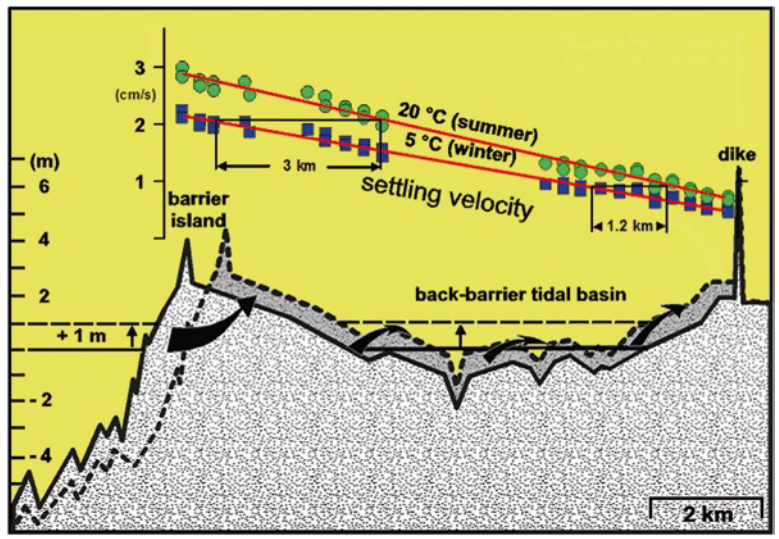

Fig. 10.3 The back-barrier energy gradient, as reflected in the progressively shoreward decreasing mean settling velocity of the sediment (Modified after Flemming 2002). Note the pronounced spatial displacement between the summer (high water temperature, low kinematic viscosity) and winter (low water temperature, high kinematic viscosity) gradient

Tidal flow patterns and suspended matter transport in back-barrier tidal basins have to date been successfully simulated over a number of tidal cycles (Stanev et al. 2007, 2009; Lettman et al. 2009). In addition, promising advances in morphodynamic modeling on decadal to millennial time scales have been made in recent years (Fortunato and Oliveira 2004; Dastgheib et al. 2008; van der Wegen and Roelvink 2008; Dissanayake et al. 2009; Ganju et al. 2009; van der Wegen et al. 2010).

As mentioned above, wave action is an important secondary hydrodynamic factor on tidal flats. Indeed, it is doubtful whether barrier islands, supratidal flats and a number of other coastal environments located above the spring high-tide level would exist at all without the influence of waves. In the case of back-barrier tidal flats, longer-period open ocean swells ($T > 8$ s) and wind waves ($T = 4–7$ s) penetrating tidal inlets loose as much as 95% of their energy through friction and breaking when crossing the ebb-deltas (Lettmann et al. 2009). As a consequence, back-barrier sedimentary processes are more strongly influenced by locally generated short-period wind waves ($T = 2–3$ s). This is reflected by the preponderance of small-scale wave ripples in both intertidal sand and mud deposits (Davis and Flemming 1995).

10.3 Morphology, Sedimentology and Mass Physical Properties

10.3.1 Morphological Characteristics

Back-barrier tidal basins are typically bounded by barrier islands on the seaward side and the mainland coast on the landward side. Laterally they are separated from neighbouring tidal basins by slightly elevated watersheds (tidal divides). The location of the watersheds depends on the angle of approach of the tidal wave relative to the orientation of the coast. If the tide approaches normal to the coast, the watersheds are located midway between the two heads of the islands. However, the more acute the angle of approach, the stronger the displacement of the watersheds in the direction of tidal wave propagation. In the case of Fig. 10.4, for example, the tidal wave approaches from the left (west), as a consequence of which the watersheds are displaced toward the right (east). As a rule of thumb, the watersheds are located where two separating flow paths at the head of the tidal wave meet at high tide behind the islands after having travelled roughly equal distances through adjacent inlets.

Individual back-barrier tidal basins are composed of a number of characteristic morphological elements.

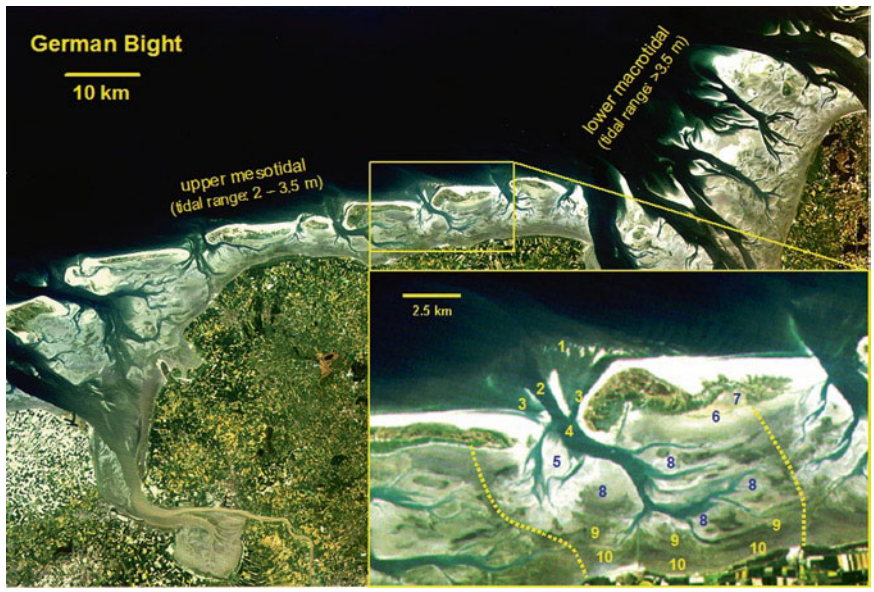

Fig. 10.4 Typical morphological elements of a barrier island depositional system, here illustrated by an example from the German Wadden Sea. *1* ebb-delta, *2* main ebb channel, *3* marginal flood channels, *4* inlet with back-barrier channel system, *5* flood ramp, *6* overwash fans, *7* back-barrier salt marsh and microbial mats, *8* sand flats, *9* mixed flats, *10* mud flats, *yellow dotted line*: tidal watersheds

This is illustrated by an example from the Wadden Sea (Fig. 10.4, inset). The depositional system begins on the seaward side of an inlet with an ebb-delta shoal (marked 1 in the inset of Fig. 10.4), which is subdivided by a central ebb channel (2) and marginal flood channels (3) that converge on the inlet (4). Inlets typically reach depths of 15–30 m, in exceptional circumstances up to 50 m, the depth being highly correlated with the tidal prism (Oost and de Boer 1994; van der Spek 1995). The same relationship applies to any location of the intra-basin channels and the fractional tidal prism discharging through that location (van der Spek 1995). In many respects the tidal channel systems comply with the morphometric rules known from fluvial drainage systems (Hack 1957; Leopold et al. 1964; Flemming and Davis 1994; Rinaldo et al. 2004).

The tidal drainage systems are cut into what are known as the back-barrier tidal flats. These can be subdivided into a number of morpho-sedimentological units that reflect particular hydrodynamic processes, in particular the shoreward decreasing energy gradient. As evident from Fig. 10.4, the intertidal flats at low tide occupy a much larger area than the tidal channels, a feature that distinguishes these systems from back-barrier lagoonal systems where the water-covered area at low tide is much larger than that of the fringing intertidal flats. It is possibly due to this fact that the type of back-barrier tidal flat system discussed here (cf. Fig. 10.4) does not display morphologically distinct flood deltas *sensu* Hayes (1979). They are instead replaced by 'flood ramps' (5) located along the outer margins of tidal-flat sand bodies facing the inlet. These ramps are barely visible on the ground but can be clearly identified on aerial photographs or satellite images by their lobate or crescentic shapes and the lighter colour of the sediment that is typical for highly mobile, drained sand that is almost devoid of biological activity. In contrast to classical flood deltas, flood ramps represent the current- and wave-reshaped margins of tidal flat sand bodies opposite the inlet.

The tidal flats and salt marshes in the rear of the islands are shaped by overwash fans (6) composed of beach sand transported across the islands during storms. On the aerial photograph in Fig. 10.5, two generations of such fans can be seen. The larger ones stem from storm events at a time when the facing part of the island was occupied by a bare supratidal flat without a protective eolian dune belt (pre-1962). Overwash activity during storms was thus unimpeded, resulting in large fans. After the establishment of a dune belt,

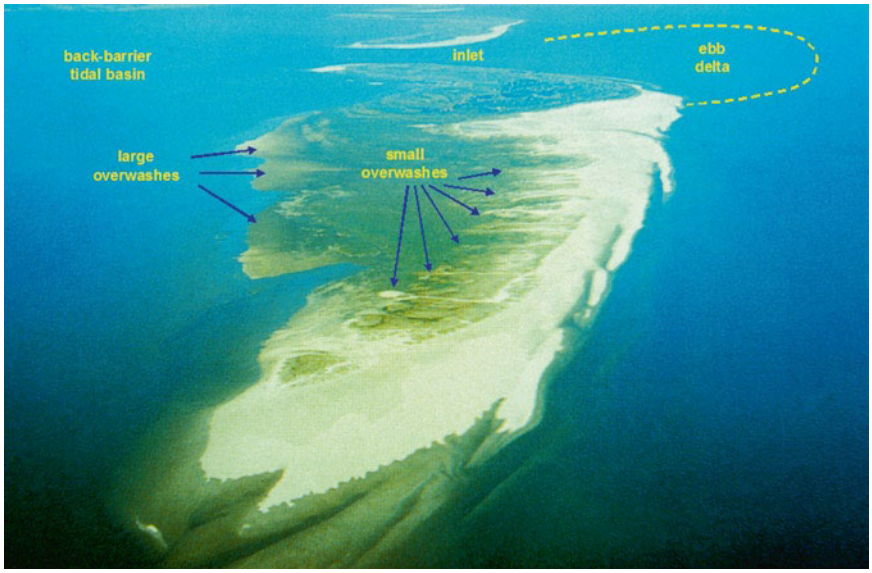

Fig. 10.5 Aerial view of a barrier island showing the location of overwash fans (Spiekeroog island, East Frisian Wadden Sea). Note the large fans that formed without obstruction of an eolian dune belt (here pre-1962) in comparison to the much smaller fans that formed after the establishment of the dune belt (post-1962)

salt marshes (7 in inset of Fig. 10.4) rapidly spread eastward and overwash activity thus became channelized through breaches in the dune belt, resulting in a larger number of smaller fans terminating in the salt marshes. Of particular interest here is the remarkably regular spacing of the breaches, which suggest a genetic link with resonant processes in the surf zone (Flemming and Davis 1994). The lobate overwash splays on the upper tidal flats are not very thick and hence difficult to identify on the ground. However, besides clear evidence on aerial photographs (e.g., Fig. 10.5), they can also be recognised by their grain-size composition, which is essentially identical to that of the adjacent beach sand (Flemming and Ziegler 1995). Within the back-barrier salt marsh, recent overwash activity is highlighted by distinctly laminated, decimetre thick sand layers penetrated by the stems and roots of salt marsh plants.

Toward the mainland shore follow the tidal flats proper. These comprise sand flats (8), mixed flats (9) and mud flats (10) (cf. Fig. 10.4). While the margins of sand flats slope more steeply toward the channels, they are almost level some distance away at elevations just below mean sea level. Along many channel margins, sand flats display slightly elevated levees formed by the interaction of tidal currents and wave action. Mixed flats and mud flats, by contrast, gradually rise toward the mean high water mark, convex profiles indicating accretion, concave ones erosion (Kirby 2000). As illustrated in Fig. 10.3, this sedimentary facies progression is hydrodynamically finely tuned, the energy gradient being associated with a progressive reduction in particle settling velocity.

10.3.2 Sedimentological Characteristics

In addition to indicators for emergence, the most striking feature of tidal flats is the pronounced shoreward fining in grain size. In effect this means that grain-size distributions gradually shift from coarser to finer mean diameters (Bartholomä and Flemming 2007), settling velocity data being generally more sensitive than sieve data because of the hydraulic sorting process (Flemming 2007). This shift in mean grain size implies a gradual change in the textural composition of the sediments. In order to describe such sediments in a consistent way, a variety of classification schemes have been devised, ternary sand/silt/clay diagrams having been the most commonly used ones (Shepard 1954; Folk 1954). Because the determination of silt and clay content is technically demanding, a simpler two-component classification based on routinely determined mud content has recently been proposed by Flemming (2000).

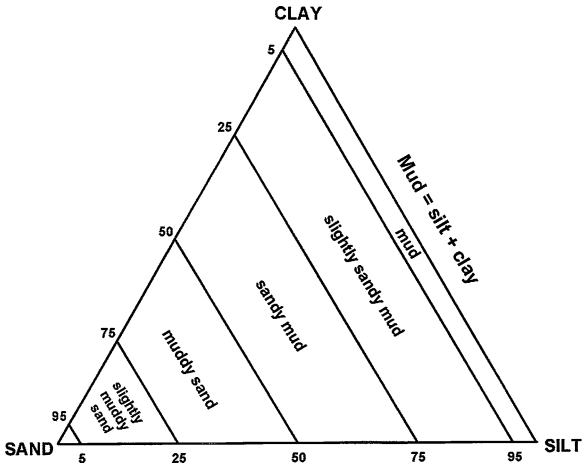

Fig. 10.6 Sediment classification based on sand/mud ratios (After Flemming 2000)

It allows the distinction of six sediment types (Fig. 10.6). These are: sand (<5% mud), slightly muddy sand (5–25% mud), muddy sand (25–50% mud), sandy mud (50–75% mud), slightly sandy mud (75–95% mud), and mud (>95% mud). The scheme provides a good spatial resolution of textural sediment composition, the textural classes also forming good descriptors of sedimentary environments or facies. For example, an intertidal area consisting of muddy sand would be called a 'muddy sand flat' or a 'muddy sand facies', etc. A more detailed scheme based on sand/silt/clay ratios, constructed by adding lines to the diagram of Fig. 10.6 fanning out from the sand endmember toward the silt-clay baseline, can be found in Flemming (2000).

In the past, it was generally thought that mixed sediments were immature, being principally more poorly sorted than sand. In recent years, however, it has been recognised that mud is composed of two major particle groups, one comprising non-cohesive 'sortable' silt (McCave et al. 1995) consisting of particles coarser than about 8 μm (medium, coarse and very coarse silt), the other comprising flocs and aggregates consisting of particles finer than about 8 μm (fine silt, very fine silt, and clay) (Chang et al. 2007). The aggregated nature of suspended sediment is illustrated in Fig. 10.7, in which a laser-based *in situ* size distribution (a) is compared with that of a dispersed sample (b) collected at the same location.

As the aggregates also get size-sorted according to the principle of hydraulic equivalence, they are deposited together with mineral grains (sand, sortable silt) having similar settling velocities. Field evidence suggests that the largest aggregates have equivalent 'grain sizes' corresponding to sand grains about 180 μm in diameter (fine sand) (Chang et al. 2007). As a consequence, the mud content of the sediment gradually increases toward finer-grained sediments in accordance with the rapidly increasing number of smaller aggregates having lower settling velocities than the larger ones. Once deposited, the aggregates are mixed into the ambient sediment, which will become increasingly more cohesive once the clay content of the total sediment exceeds 5–10% (van Ledden et al. 2004). Laboratory analyses of dispersed mud thus introduce mechanical artefacts into grain-size distributions that suggest poor sorting. In hydraulic terms, such sediments are actually very well sorted, the standard deviation of the sand fraction being a good approximation of the 'true' sorting of the total sediment. The deposition of mud on tidal flats is thus controlled by the settling velocities of the differently sized flocs and aggregates and not by those of the constituent particles. At a water temperature of 18°C the critical lower size limit for individual 'sortable' silt particles (8 μm) corresponds to a settling velocity of ~0.01 cm s^{-1}, smaller particles being rapidly scavenged to be incorporated into aggregates ranging from floccules to fecal pellets. Conceptually this is in excellent agreement with earlier findings about the settling velocity of suspended matter in a variety of environments (Nichols and Biggs 1985, based on data of Migniot 1968; Haven and Morales-Alamo 1968; Owen 1971, and Krone 1972) (Fig. 10.8).

The diagram in Fig. 10.8 shows the settling velocity range of dispersed clay particles at 18°C relative to that of composite particles (flocs and aggregates) in quiet and turbulent water, as well as that of fecal pellets. The corresponding equivalent grain size of quartz spheres shows that the bulk of aggregated material generally exceeds the critical size, fecal pellets and some of the flocs and aggregates being hydraulically equivalent to grain sizes as large as fine sand. While sortable silt particles, as in the case of sand, respond in a predictable way to changing hydrodynamic conditions, flocs and aggregates constantly change their size and composition in the course of transport, deposition and resuspension due to continually changing shear forces in the course of a tidal cycle (Chang et al. 2006b). Because the number of aggregates increases

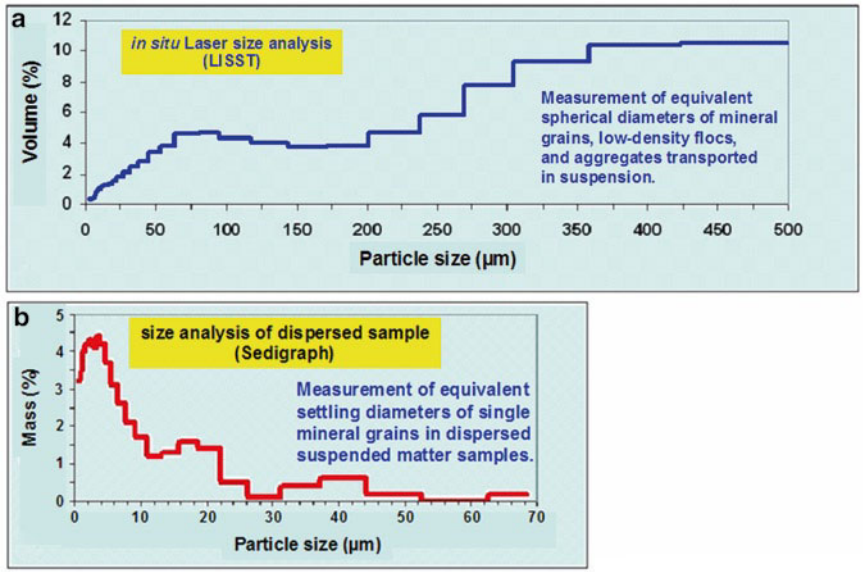

Fig. 10.7 Comparison of particle-size distributions carried out *in situ* on suspended matter by means of a laser particle sizer (**a**) and in the laboratory by means of a Sedigraph™ (**b**). In the latter case, the analysis was carried out on a disaggregated (dispersed) sample collected at the same site (Based on Chang et al. 2007). It is clearly evident that the bulk of the suspended material consists of a wide range of differently sized aggregates which, when disaggregated, is seen to be primarily composed of constituent particles <10 µm in size

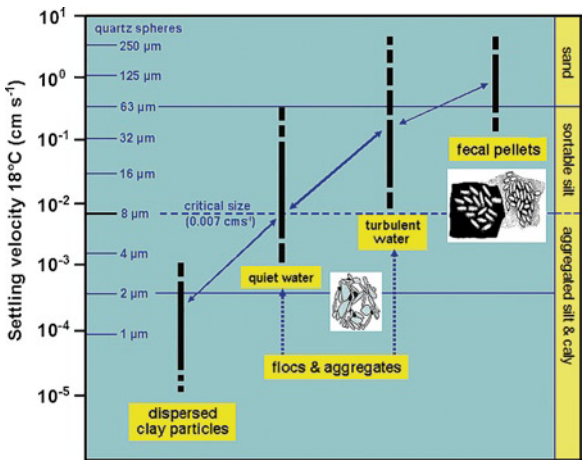

Fig. 10.8 Settling velocities and corresponding grain sizes of hydraulically equivalent quartz spheres of dispersed clay particles, flocs and aggregates in quiet and turbulent water, as well as fecal pellets (Modified after Nichols and Biggs 1985; based on data of Migniot 1968; Haven and Morales-Alamo 1968; Owen 1971; and Krone 1972). Note that the bulk of aggregated material exceeds the critical size of 8 µm. The *arrows* indicate continuous exchange in the course of aggregation and disaggregation in response to changes in current shear and bioactivity

rapidly with decreasing size, the gradual increase in mud content in the direction of the energy gradient is plausibly explained.

The partitioning of mud into two fundamentally different particle groups challenges the conventional wisdom of plotting sand/silt/clay ratios in ternary diagrams and suggests that important information may also be gained from plotting the ratios of sand, sortable silt (8–63 µm fraction), and flocs & aggregates (<8 µm fraction). This is illustrated by the two comparative plots in Fig. 10.9 that were generated from the same Wadden Sea dataset. While the conventional plot (a) shows a silt-clay partitioning at proportions of about 37–63%, the modified plot (b) reveals that, in this particular example, sortable silt and aggregated material contribute about equal amounts to the mud fraction of the back-barrier tidal basin.

The ternary diagrams in Fig. 10.9 show that sediment composition in back-barrier tidal basins is represented by narrow bands extending across the entire spectrum of sedimentary facies from sand to mud as defined in Fig. 10.6. Such trends are typical of many

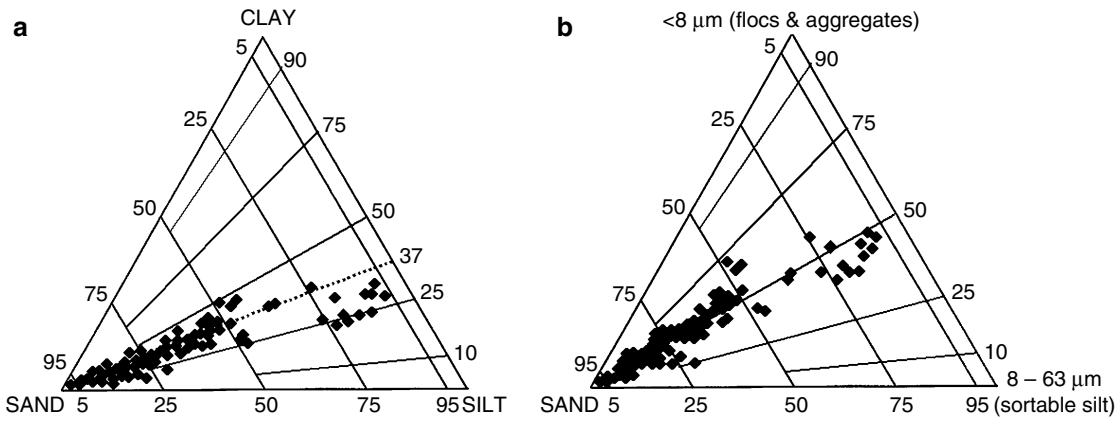

Fig. 10.9 Ternary diagram of sand/silt/clay ratios (**a**) and sand/sortable silt/flocs & aggregates (**b**) observed in a back-barrier tidal basin of the German Wadden Sea. Note the 50/50 partitioning of sortable silt and aggregates in the latter case, as opposed to a 63/37 partitioning of silt and clay in the former case (Based on Chang et al. 2007; subdivisions after Flemming 2000)

mixed sedimentary environments (Flemming 2000). At the same time the progression reveals energy gradients from sand to mud, on one hand, and between silt and clay, on the other (cf. Pejrup 1988; Molinaroli et al. 2009). In diagram a, the position of the data band between the silt and clay endmembers suggests a relatively exposed depositional environment, whereas in diagram b it occupies a more intermediate energy position. Which of the diagrams is hydraulically more relevant in this context requires further investigation as comparative data for the case b are currently lacking. Nevertheless, in both cases the grain-size composition allows a relative energy classification of the environment (Flemming 2000; Molinaroli et al. 2009).

10.3.3 Mass Physical Sediment Properties

Sedimentary environments such as back-barrier tidal flats are highly dynamic systems that constantly change their outward appearance in response to energy fluctuations, on a regular basis in the course of the spring-neap tidal cycle and episodically by sediment reworking during storms. To quantify such changes, the import and/or export of material to or from a tidal flat area is commonly achieved by repeated elevation surveys with subsequent calculation of volume changes between surveys. The volume changes then need to be converted into material masses. This is achieved by determining critical mass physical sediment properties. Important parameters in this context are wet and dry bulk densities, porosity, water content, and organic matter content. Mass balancing exercises are particularly important in disciplines such as sedimentology, geochemistry, biology, microbiology, and biochemistry. Good examples can be found in Bartholomä et al. (2000) for the import and export of sand and mud, and in Delafontaine et al. (2000) for organic matter.

In tidal flat environments, both wet and dry bulk density have been found to be highly correlated with mud content and average values of the former can thus be calculated from the latter on the basis of regression analyses. Examples from the Wadden Sea are shown in Fig. 10.10. From the calibration curves it can be seen that pure sand has an average wet bulk density (BD_w) of ~2.0 g cm^{-3} and a corresponding dry bulk density (BD_d) of ~1.6 g cm^{-3}. At the other end, the wet and dry bulk densities of pure mud are ~1.2 and ~0.3 g cm^{-3}, respectively. More precise average values can be calculated on the basis of the regression equations. Although the Wadden Sea trends should be generally valid for many other tidal flat systems composed of terrigenous material (quartz, feldspar, rock fragments, carbonate, clay minerals), it is nevertheless advisable to establish separate calibration curves for other areas, especially if organic matter contents are high (Delafontaine et al. 2004).

Wet and dry bulk densities can also be determined from the water content (Wc) of intertidal sediments. An example for dry bulk density is illustrated in Fig. 10.11.

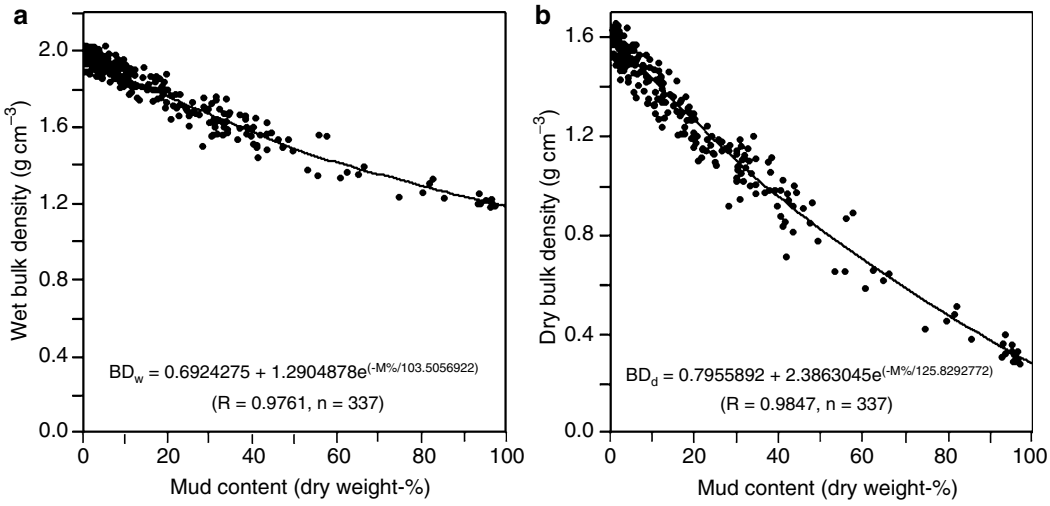

Fig. 10.10 Relationship between mud content and wet (**a**) and dry (**b**) bulk densities in Wadden Sea sediments (Based on Flemming and Delafontaine 2000)

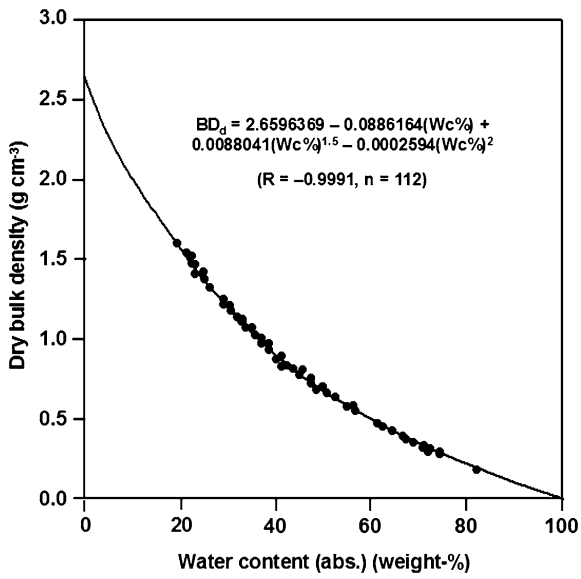

Fig. 10.11 Relationship between dry bulk density and absolute water content in intertidal sediments of the Wadden Sea (Based on Flemming and Delafontaine 2000). Note the very high correlation. The relationship has universal character for average terrigenous material

As can be seen, the correlation is superior to that for mud content (Fig. 10.10b) and, for average terrigenous material ($\delta = 2.65$ g cm^{-3}), this relationship has universal character (cf. regression equation in Fig. 10.11). It is important, however, to carefully distinguish between absolute and relative water contents, the former being defined as the ratio between the mass of pore water and the mass of the total water-saturated sample, the latter as the ratio between the mass of pore water and the mass of the dry solids. Relative water content can reach several hundred percent, i.e. the mass of the water can greatly exceed the mass of the dry solids, whereas the absolute water content is always a fraction of one-hundred. Relative water content <100% can therefore be confused with absolute content if not identified as such. Excellent treatments of these and other mass physical properties can be found in Lambe and Whitman (1969), Carver (1971), Inderbitzen (1974), Dunn et al. (1980), Hillel (1998), and Warrick (2002).

Mass concentrations of sand and mud relative to the total sediment (sand + mud) are illustrated in Fig. 10.12a. Of particular interest here is the counter-intuitive trend described by the dry mass concentration of the mud component (Fig. 10.12b). Thus, with increasing mud content, the mass concentration of mud initially increases as would intuitively be expected. At higher mud content, however, the trend changes in an unexpected manner, i.e. it flattens off, peaks (in this case at a mud content of about 60%), and thereafter decreases again. This counter-intuitive trend is caused by a progressive change in the network structure or fabric of the sediment as the water content increases with increasing mud content. Beyond the apex of the

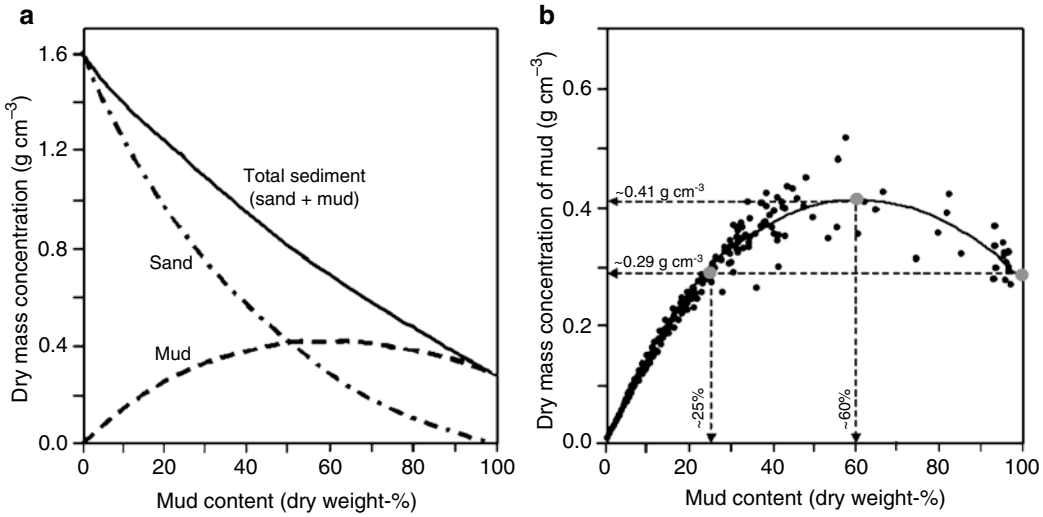

Fig. 10.12 Dry mass concentrations of sand and mud relative to the total sediment (**a**). Note the counter-intuitive trend in the progression of the mud component (**b**) which reverses after peaking around 60% in this dataset from the Wadden Sea (Based on Flemming and Delafontaine 2000)

regression curve, the network structure is very loose, being merely supported by flocs and aggregates. As sand is added, the grains initially fill the voids by expelling water without breaking down the network structure that results in a proportional increase in the mass concentration of mud. This continues up to the apex point where the sand content in this case is about 40%. As this limit is approached, the network structure begins to break down and the sediment is increasingly grain supported, water and mud now filling the voids between the sand grains. In effect this means that, in a unit volume of intertidal sediment, the mass concentration of mud in sediment consisting of pure mud (>95% mud content) is equal to that at mud contents as low as 25%, while the highest mass concentration of mud is registered at the apex of the regression curve. As in the case of bulk density, other tidal flat environments may have slightly different trends to the Wadden Sea example shown here. If required, corresponding calibration curves should therefore be established for other tidal flat environments.

The unexpected trend observed in mud mass concentration has far-reaching implications because any other parameter linked to the mud fraction (e.g., organic matter, trace elements, pollutants) will by necessity follow a similar trend. Contrary to common perception, highest mass concentrations of mud, and hence of any substances linked to the mud fraction, are found in mixed sediments (muddy sand and sandy mud) and not in pure mud. This potentially confusing issue and its pitfalls are discussed in detail by Flemming and Delafontaine (2000). A particularly common mistake is to relate measures of concentration, i.e. masses per unit volume or area, e.g., animal density per m^2, to measures of content, i.e. masses per unit mass, e.g. weight-% organic matter. By ignoring the dimensional incompatibility between contents and concentrations, it goes unnoticed that corresponding masses occupy increasingly larger volumes as the water content and the mud content increases. Thus, the volume occupied by a unit mass of pure mud with a dry bulk density ~0.3 g cm^{-3} is more than five times larger than that occupied by the same mass of pure sand having a dry bulk density ~1.6 g cm^{-3}. For organic carbon, which is a measure commonly associated with the amount of food available to organisms, this disparity is illustrated in Fig. 10.13. The positive correlation between POC content and mud content (Fig. 10.13a) is commonly assumed to indicate that the largest amount of food is contained in pure mud as reflected by the highest POC content. However, as in the case of mud mass concentration (Fig. 10.12b), the relationship between POC mass concentration and mud content (Fig. 10.13b) clearly demonstrates that this assumption is wrong, the amount of POC per unit volume of sediment that corresponds to the dimensional measure for animal

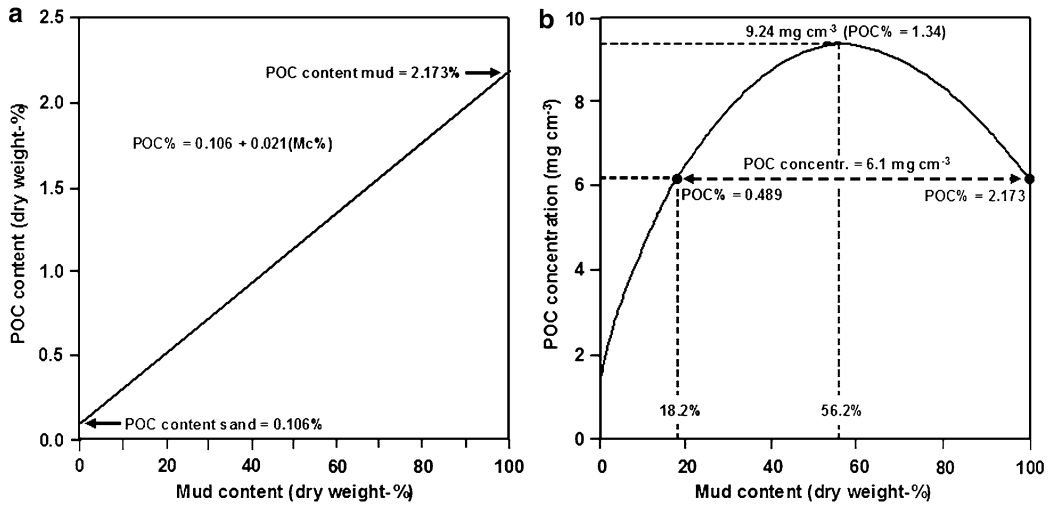

Fig. 10.13 Comparison of the trends in organic carbon content (**a**) and organic carbon concentration (**b**) as a function of mud content (data points omitted for clarity) (Based on Flemming and Delafontaine 2000). Note the similarity of the POC concentration curve to that of mud mass concentration in Fig. 10.12b

density being identical at 18% mud content, and up to 50% larger at intermediate mud content, in comparison to that at 100%. As pointed out earlier, this would also apply to any other sediment component linked to the mud fraction, e.g. heavy metals, trace elements, organic pollutants, toxic substances.

A mass physical property of intertidal sediment that plays an important role in the mobility or stability, i.e. the erosion resistance, of sediment, is the shear strength of the substrate. This parameter is conveniently determined in the field by a so-called vane shear apparatus where cross-vanes of different dimensions are calibrated such as to provide the shear strength upon yield after being inserted into the sediment and twisted against the resistance of a spring. Shear strength of intertidal sediment in relation to mud content, porosity, wet bulk density, and dry bulk density is illustrated in Fig. 10.14. Overall, the shear strength of intertidal sediment decreases with increasing mud content and porosity, and consequently increases with increasing wet and dry bulk density. Two features in the illustrated trends are of particular interest here. First, in all four cases, the highest and lowest shear strength for any value of the other parameter is well defined in what could be called an upper and lower boundary criterion. Both have a similar positive or negative trend as the mean trend line that would be defined by a regression analysis. In the case of mud content this means that for each of the criteria (i.e. upper boundary, mean, lower boundary) the shear strength progressively decreases as mud content increases, the reverse being true for bulk density. This applies in corresponding manner to any other correlating parameter.

The other interesting feature is the increasing range in shear strength (increasing standard deviation) toward lower mud content and porosity, and higher bulk density. The increasing scatter of the data points reflects an increasing variability in the degree of compaction (grain packing density) toward more sandy sediments. This is not unexpected as the hydrodynamic energy also increases toward higher sand content. The trends therefore trace the shoreward energy gradient together with its local variability, which is highest in sand. Thus, wave-compacted sands will have relatively high shear strength, whereas waterlogged sand will display a shear strength that may be as low as that at intermediate to high mud content. Excluded from these examples is dewatered mud commonly found in the subsurface of mixed flats, in channel-fill sequences, and between the neap and spring high-tide level where desiccation over the neap-tide period results in compaction and corresponding higher bulk density associated with lower porosity and water content.

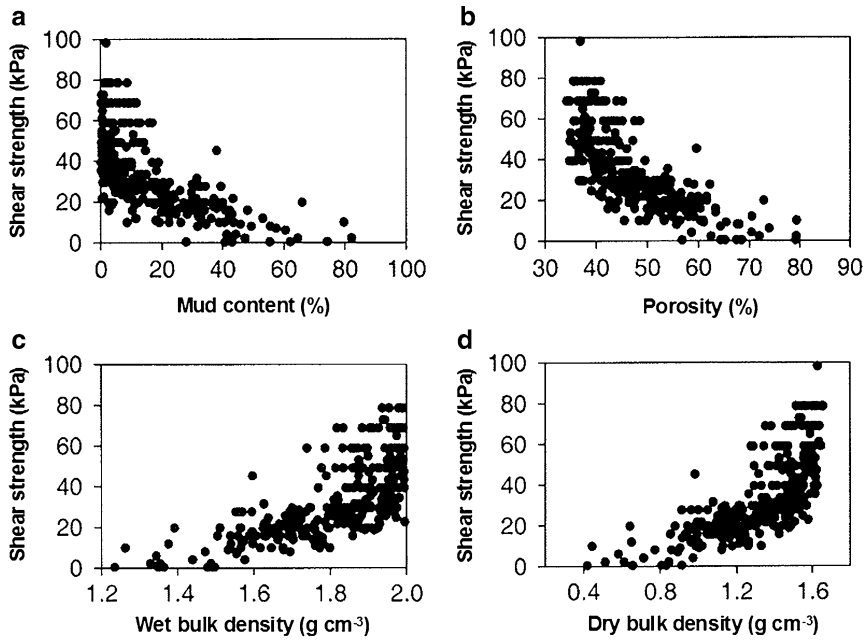

Fig. 10.14 Shear strength as a function of mud content (**a**), porosity (**b**), wet bulk density (**c**), and dry bulk density (**d**). Note the clearly defined maximum and minimum shear strengths for any value of the given parameters, and the increasing range (standard deviation) in shear strength with decreasing mud content and porosity, but increasing bulk density (Based on Xu 2000)

10.4 Depositional Facies and Sedimentary Structures

Barrier island depositional systems include a variety of facies that are intimately related to the morphological elements illustrated in Fig. 10.4. In the course of vertical accretion, the individual facies take on the form of three-dimensional, interfingering sedimentary units that define the internal architecture of the depositional system. In Fig. 10.15, the most important sedimentary units of back-barrier tidal flats are illustrated in a schematic geological cross-section of a Holocene barrier system (Fig. 10.15) that is aligned perpendicular to the shore and cuts through the middle section of a typical barrier island system of the Wadden Sea. Similar examples can be found in van Straaten (1964), Reineck and Singh (1980), Beets et al. (1996), and Vos and van Kesteren (2000).

The base of the depositional system is commonly formed by an erosional unconformity (here above Pleistocene deposits). In some places, pre-existing and partly eroded brackish-water deposits and basal peat can still be found. On the seaward side, the barrier system commences with shoreface/beach/eolian dune or shoreface/ebb-delta/inlet deposits not shown here, depending on where the cross-section is located relative to the barrier shoreline. The bulk of the back-barrier depositional system consists of channel fills and tidal-flat deposits, the latter getting progressively finer-grained toward the mainland shore. The land-sea transition is commonly marked by extensive salt marsh deposits. In the immediate rear of the coastal barriers, salt marshes and overwash deposits complete the depositional sequence. Intercalated brackish-water deposits and peat horizons may occur up to variable distances from the mainland shore, indicating temporary sea-level still-stands or short-lived regressions. Superimposed on this depositional system is a variety of biofacies comprising particular invertebrate animal communities adapted to exist in particular parts of the system (Frey and Howard 1969; Schäfer 1972; Howard and Frey 1975; Hertweck 1994). In addition to depending on the geographic (climatic) location, the community structure also depends on the energy gradient (current and wave exposure), on the tidal gradient (exposure or immersion period), and on sediment composition, including organic matter (food resources). Many of

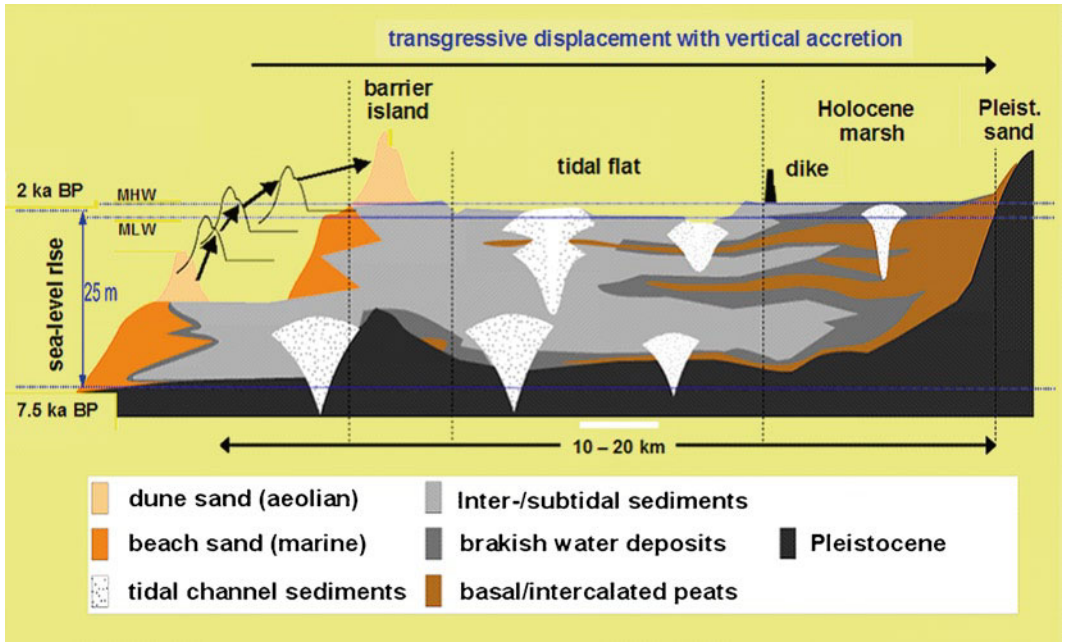

Fig. 10.15 Schematic geological cross-section through a transgressive barrier island depositional system as exemplified by the Wadden Sea and showing typically stacked sedimentary facies relating to particular coastal environments and facies (Modified after Streif 1990)

these organisms are shell-producing and hence contribute to the total and bioclastic material budgets of the back-barrier depositional system. In addition, most of the organisms are responsible for a partial or complete destruction of primary sedimentary structures up to the depth of their burrowing and feeding activity. This 'bioturbation' process also includes the activity of some higher order animals such as birds and fish.

In a geological context, bioturbation and the production of bioclastic material are tidal flat attributes that have only evolved in the course of the Phanerozoic (600 Ma BP – Present), older (Precambrian) deposits being generally devoid of such features. Finally, any list of biological influences would be incomplete if algal and bacterial activity were omitted. In this context, true algal mats, which consist predominantly of green algae and mostly occur on muddy tidal flats and in salt marsh pools, must be distinguished from mats produced around the mean high-water level by so-called 'blue-green algae' (cyanobacteria). These latter mats should correctly be referred to as 'microbial' mats (e.g., Gerdes and Krumbein 1987; Noffke 2010).

At smaller spatial scales, the basic depositional building blocks of back-barrier tidal flat systems outlined above are characterized by a large variety of physical and biological surface structures as well as internal sedimentary structures which, if comprehensively illustrated, would fill a whole book. Good summaries of typical clastic tidal facies and their sedimentary structures can be found in de Raaf and Boersma (1971), Klein (1977), and Reineck and Singh (1980), while biogenic structures and ichnofacies of temperate tidal environments are comprehensively dealt with in Schäfer (1972). For the purpose of this contribution, a selection of features is presented that, alone or in combination, have some degree of diagnostic power in identifying tidal flat deposits in the rock record.

10.4.1 Biological Surface Structures

The evolution of organisms in the course of the Phanerozoic, and their frequent adaptation to specific environmental conditions, has greatly facilitated the identification of particular depositional environments in the rock record. Intertidal flats are no exception in this context.

In Fig. 10.16a, a well preserved and still rooted tree stump in the middle of an intertidal flat suggests transgressive inundation in the East Frisian Wadden

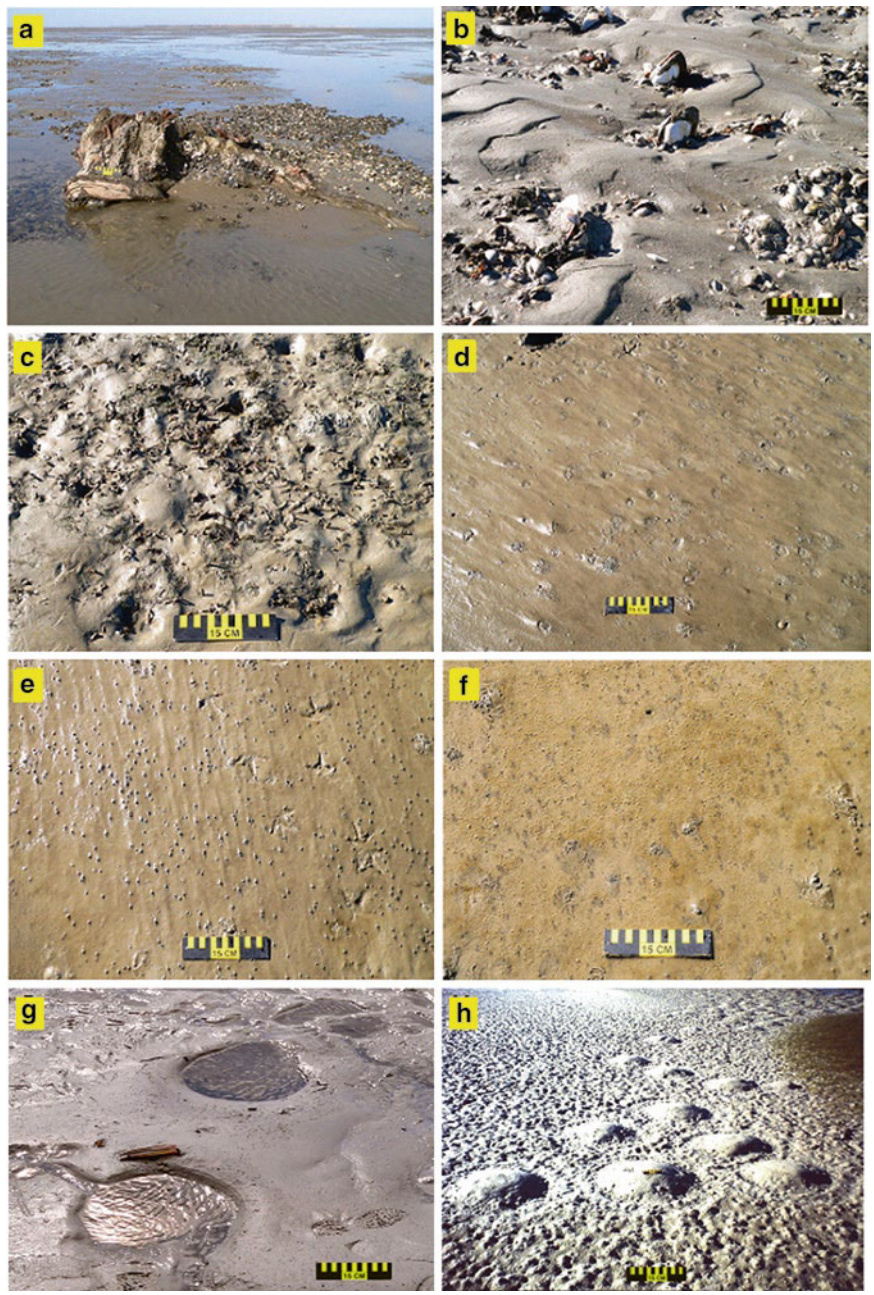

Fig. 10.16 Evidence for biological activity on tidal flats. (**a**) Rooted tree stump; (**b**) Shell lag together with articulated bivalve shells in live position (*Mya arenaria*); (**c**) Protruding polychaete tubes (*Lanice conchilega*) together with bird tracks and crawling traces of intertidal snails; (**d**) Sandy mud flat colonised by juvenile bivalves (*Cerastoderma edule*) living just beneath the sediment surface. Note bird track at the top and the uniformly aligned mounds and streaks indicating current flow from lower right to upper left; (**e**) Muddy sand flat with small polychaete fecal mounds (*Heteromastus filiformis*). Note the bird tracks and the current-aligned streaks emanating from the fecal heaps (current from bottom to top); (**f**) Slightly muddy sand flat colonised by *Arenicola marina* (large stringy fecal heaps) and *Heteromastus filiformis* (small *gray* fecal patches). Note patches of diatoms (*brownish discoloration*) producing gas bubbles (oxygen); (**g**) Feeding hollows created by trampling seagulls; similar hollows are made by rays; (**h**) Feeding hummocks created by flamingos (here in Langebaan Lagoon, South Africa)

Sea, Germany. Of similar diagnostic potential are organisms that only occur in intertidal environments, especially when preserved in live position such as the bivalve *Mya arenaria* in Fig. 10.16b. More difficult to assign to a tidal flat setting are organisms that also live subtidally. In such cases, additional evidence is required to diagnose an intertidal setting. The polychaete *Lanice conchilega* in Fig. 10.16c is a case in point. It is only in conjunction with other diagnostic criteria such as bird tracks that an intertidal setting can be allocated with some degree of confidence. The same applies to the cockle or heart mussel (here *Cerastoderma edule*) that lives just below the sediment surface and that can be recognised by the bumpy surface or the scars produced by slightly protruding shells (Fig. 10.16d). Similarly, while the presence of the polychaete *Heteromastus filiformis* is betrayed by the occurrence of small (black or gray) fecal heaps on the surface of modern tidal flats (Fig. 10.16e), it would be the bird tracks on the same bedding plane that would identify the depositional environment as being intertidal in the rock record. In principle this also applies to the lugworm *Arenicola marina* (Fig. 10.16f), here in community with *Heteromastus*. Circular resting hollows of rays or feeding hollows of wading birds (Fig. 10.16g, here seagulls) and feeding hummocks created by flamingos (Fig. 10.16h, here in Langebaan Lagoon, South Africa) complete the picture.

Considering that large-scale exposures of fossil bedding planes are relatively rare in comparison to vertical sections, it is inherently difficult to identify intertidal settings with confidence in the rock record on the basis of surface structures alone unless additional unequivocal diagnostic evidence is available. Such evidence includes late-stage emergence runoff features and traces of organisms restricted to the intertidal, including the tracks and feeding structures of wading birds. In cold climates, such evidence would in addition encompass tool marks induced by moving ice floes. In all other cases, it would be the association of a multitude of features which, by application of the exclusion principle, could eventually justify a decision in favour of a particular environment.

10.4.2 Physical Surface Structures

Prominent physical surface structures frequently observed on tidal flats include wave and current ripples that display features characteristic of very shallow water and late-stage emergence. Prominent among these are extensive sheets of symmetrical and asymmetrical wave ripples (Fig. 10.17a). Because ripples also occur in subtidal environments, one should in addition look for evidence of late-stage emergence. Such features include ladderback ripples (Fig. 10.17b), especially where smaller trough-bound wave ripples aligned perpendicular to the larger ripple crests are associated with water-level marks (Fig. 10.17c). The small wave ripples in the troughs in Fig. 10.17c formed when the water level had dropped below the crest level of the larger ripples but before the water-level marks formed which later dissected the crests of the small ripples where they merge with the steep slopes of the larger ones.

Features formed during late-stage run-off are particularly diagnostic for emergence at low tide. Among these are narrow streams of linguoid current ripples dissecting wave-rippled surfaces, the crests of the latter having in this case been flattened just before emergence (Fig. 10.17d). Shallow, laterally migrating intertidal creeks are commonly paved by shell beds (Fig. 10.17e), in this case overlain by narrow sand ribbons formed during upper-plane-bed flow shortly before emergence. It should be noted here, however, that shell concentrations can also result from the burrowing activity of intertidal organisms, in particular *Arenicola marina* (van Straaten 1952). Near steeper channel margins, such creeks display a multitude of late-stage runoff features such as scour pits around shells, grooves, rill marks, microbars and small fan structures (Fig. 10.17f).

Wave- and current-generated ripples are frequently observed in muddy sediments upon exposure at low tide (Fig. 10.17g). This contradicts the common perception that such bedforms do not form in fine-grained sediments. Their occurrence has been explained by the aggregated nature of the mud during transport and deposition, the aggregates and also fecal pellets initially responding to waves and currents as non-cohesive particles would, similar to the fine or very fine sand to which they are hydraulically equivalent (Schieber and Southard 2009). In contrast to rippled mud, tidal flat surfaces may locally become draped by thin blankets of fluid mud (Fig. 10.17h) that often display erosional windows revealing the underlying sediment together with any surface structures on them (in this case wave ripples). An analogous feature can be observed in

Fig. 10.17 Physical surface structures frequently observed on tidal flats. (**a**) Asymmetrical wave ripples; (**b**) Ladderback ripples; (**c**) Small wave ripples in the troughs of larger ripples and water-level marks; (**d**) Late-stage runoff with linguoid current ripples dissecting a field of flat-crested wave ripples; (**e**) Shallow intertidal creek with small sand ribbons over shell pavement; (**f**) Late-stage runoff features; (**g**) Current ripples in mud; (**h**) Thin fluid mud sheet with scour windows displaying ripples on the surface of underlying sand. (**i**) Circular tool mark formed by the rotation of a protruding polychaete tube. Note the bird tracks surrounding the structure; (**j**) Rippled sand bed with patchy wash-outs formed shortly before emergence; (**k**) Intertidal dunes; (**l**) Shell pavement

sandy sediment where a rippled surface is overlain by slightly elevated, smooth-topped sand patches (Fig. 10.17j). These patches are the remnants of an eroded sand sheet that was locally stabilized by diatoms. The lower surface was subsequently covered by wave ripples, whereas the surfaces of the elevated patches were smoothed by wind-induced washover shortly before emergence.

Tool marks are less frequent than other surface structures on tidal flats but may on occasion be encountered where driftwood or dislodged algae have scraped or rolled across the sediment surface in shallow water. In contrast to this, a large variety of scour, prod and roll marks induced by drifting ice floes are ubiquitous on tidal flats in cold regions (Dionne 1974; Reineck 1976; Dionne 1988; Pejrup and Andersen 2000). A rather

unusual concentric tool mark is illustrated in Fig. 10.17i where a protruding polychaete tube has excavated a circular groove around its holdfast (diameter ca. 20 cm). Larger-scale current-generated features on tidal flats are represented by 2D and 3D dunes (Fig. 10.17k) that, in back-barrier tidal basins, are usually best developed at spring tide. Upon emergence, the dunes commonly display well-developed water-level marks along their steep slipfaces. Finally, extensive and often very selective shell beds swept together by wave action, in contrast to current-generated lag deposits, can be found locally on more exposed parts of intertidal flats (Fig. 10.17l).

10.4.3 Internal Sedimentary Structures

Reconstruction of ancient depositional environments is commonly based on the interpretation of internal sedimentary structures, bedding types, and stratification sequences observed in rock outcrops or cores. In modern environments, internal structures are either visualized by trenching and preparation of lacquer peels or, where conditions prevent this, by coring and preparation of relief casts using suitable resins (e.g., Bouma 1969). Due to the water-saturated nature of the sediments, coring is the only feasible procedure in tidal flat research. While sedimentary structures are well preserved in cores, they have the disadvantage of only revealing narrow sections of laterally more extensive structures.

In spite of this, the systematic preparation of both short box-cores since the 1950s and longer vibro-cores since the late 1970s has revolutionized our understanding of tidal flat deposits (Reineck and Singh 1980). This is illustrated in Fig. 10.18 by a small selection of relief casts ranging from exposed sand flats to protected salt marshes. As mentioned earlier, small subaqueous dunes are best developed along the ebb-dominated, outer tips of flood ramps on sand bodies facing the inlet. This is exemplified by the cross-bedding in Fig. 10.18a where the flow was dominated by the current flowing from right to left. The tangential cross-beds are indicative of 3D dunes and hence relatively strong flow as opposed to planar cross-beds indicative of 2D dunes and weaker flow. Considerably weaker and more evenly distributed bidirectional currents of uniform strength are reflected in the sequences of vertically-stacked herringbone cross-stratified units in Fig. 10.18b. The term 'herringbone' is strictly reserved for sets of ripple cross-stratified beds displaying opposing dip directions formed in the course of individual ebb-flood or flood-ebb cycles. Not all opposing cross-beds comply with this definition because individual units may be separated by hiatuses of varying duration. Furthermore, misinterpretations can result where bidirectional currents are wrongly inferred from trough cross-beds cutting each other at odd angles (Reineck and Singh 1980).

A typical stratification sequence found along shallow, migrating intertidal creeks is illustrated in Fig. 10.18c where the partly excavated and still articulated shells of *Mya arenaria* in live position protrude through a shell lag deposit that accrued as a tidal creek migrated across it. The core reflects in a remarkable way the subsurface conditions of a surface situation as illustrated in Fig. 10.16b. A second shell layer near the bottom of the core indicates the depth of the tidal creek during a previous crossing. The horizontally stratified channel fill above this layer is partly obliterated by bioturbation. Quite different are the deposits found along the margins of larger and deeper channels. Such tidal flat margins are frequently composed of horizontally laminated, partly waterlogged beds that, at depth, may be deformed into convolute beds by sudden liquefaction events (Fig. 10.18d; cf. Wunderlich 1967). In other cases, channel-margin deposits comprise small current- and/or wave-rippled cross-bedded sets (Fig. 10.18e). Convolute lamination has also been observed to form as a result of entrapped air (de Boer 1979). Processes and concepts of convolute bed formation, also including tidal flats, have been comprehensively described by Williams (1960) and Einsele (1963).

Proceeding from sand flats to mixed flats, the degree of bioturbation gradually increases (Fig. 10.18f, i). At low mud content (slightly sandy mud), ripple troughs initially get draped by thin mud layers that, in cross-section, produce the well-known flaser structures (Fig. 10.18g). As the mud content increases with decreasing energy, the mud drapes get thicker and eventually form interconnected wavy layers alternating with rippled sand layers to produce the characteristic wavy bedding around the transition between intertidal muddy sand and sandy mud facies. Finally, as the sand content decreases (sandy mud to slightly sandy mud facies), the internal sedimentary structures are now dominated by thick mud drapes interrupted by connected or disconnected sand lenses (starved ripples)

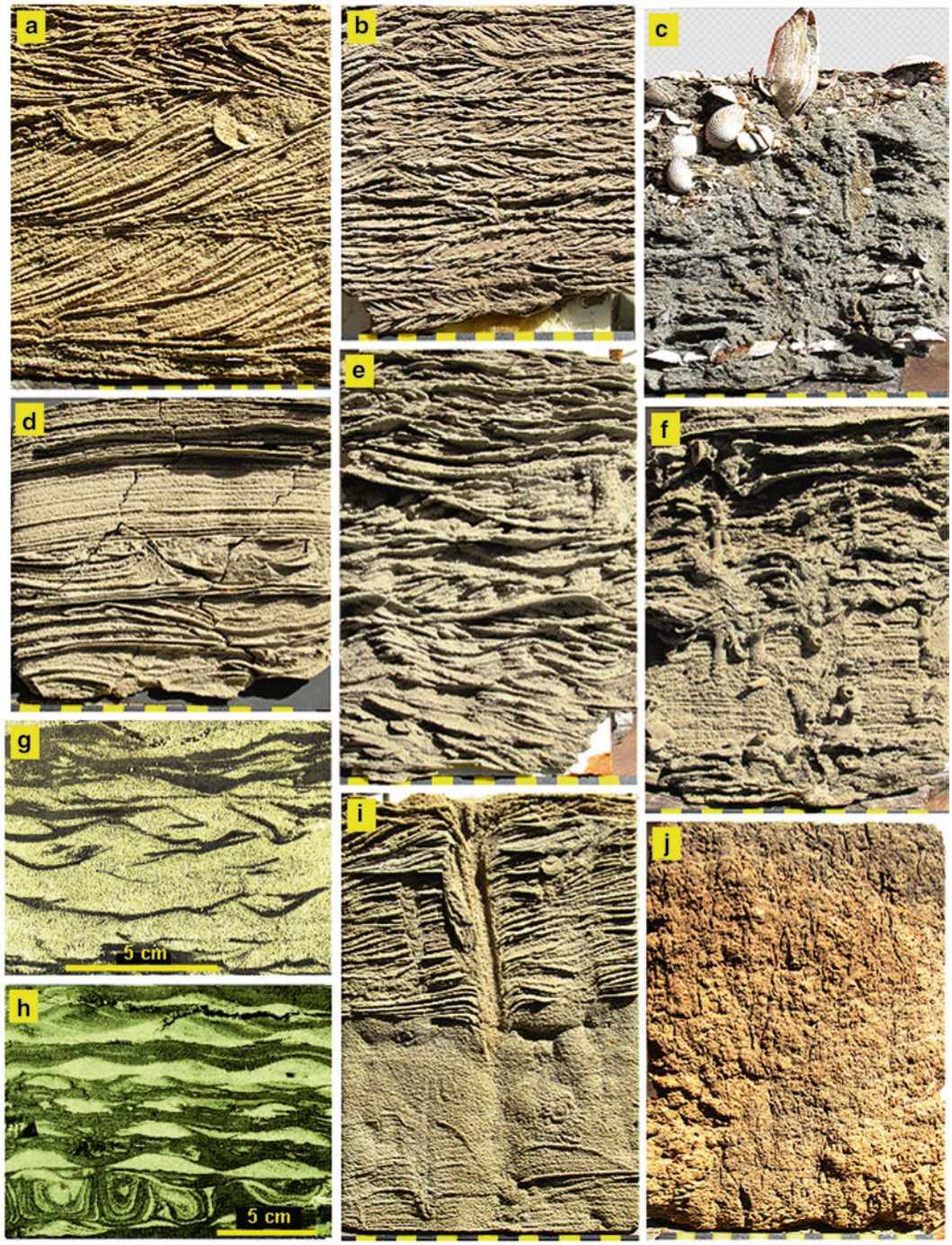

Fig. 10.18 Internal sedimentary structures typical for tidal flat deposits. (**a**) Bidirectional dune cross-bedding with current dominance from right to left; (**b**) Bidirectional ripple cross-bedding with well-developed herringbone structures; (**c**) Partly bioturbated sand with shell layer at depth and shell lag at the surface. Note partly excavated shell of the bivalve *Mya arenaria* in live position; (**d**) Horizontally bedded sands above several convoluted bedsets; (**e**) Multidirectional wave and current ripples in sand. Note the absence of clear herringbone structures; (**f**) Partly bioturbated, horizontally bedded sand in lower part of core, grading into partly bioturbated rippled sand in upper part; (**g**) Flaser bedding typical for muddy sand facies; (**h**) Lenticular bedding typical for sandy mud facies; (**i**) Weakly laminated sand in lower core, followed by well preserved lamination in upper core, both penetrated by a large worm tube, possibly of *Arenicola marina* (u-part hidden); (**j**) Rooted salt marsh deposit

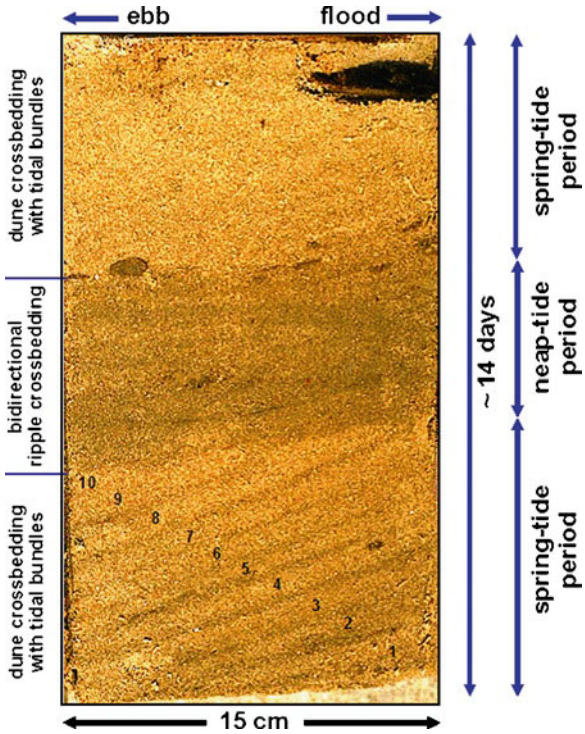

Fig. 10.19 A vertically stacked spring-neap-spring cycle with tidal bundles preserved in intertidal dune cross-beds formed over spring tide. The bundles are clearly visible in the *bottom sequence*, but only faintly so in the *upper* one. Note that the bundles are not separated by mud drapes, but instead by finer-grained sand

to form so-called lenticular bedding (Fig. 10.18h, cf. Reineck and Wunderlich 1968. Flemming 2003a). Due to the high water content of the mud, overburden pressure can result in the formation of convolute bedding in this environment (Fig. 10.18h, bottom). Pure mud is either completely homogenized or thinly laminated, depending on the degree of local bioturbation. These eventually grade into salt marshes, the laminated deposits of which are usually intensely bioturbated by root structures (Fig. 10.18j).

The cores illustrated in Fig. 10.18 do not include any evidence of tidal bedding such as sand-mud couplets or tidal bundles associated with deposition in the course of neap-spring cycles. Such rhythmic sedimentary structures are well documented from subtidal channels (Visser 1980; Allen and Homewood 1984) and from estuarine mudflats in macrotidal settings (Dalrymple et al. 1991), but have rarely been reported from back-barrier tidal flats. A cross-bedded example from the Wadden Sea is presented in Fig. 10.19.

The box-core was recovered from a dune of the type shown in Fig. 10.17k. It is interpreted to show a vertically-stacked spring-neap-spring sequence with clearly visible tidal bundles in the crossbeds of the lower unit and more faintly preserved ones in the upper unit. The two units were formed during the ebb tide over successive spring-tide periods and are separated by a bipolar, current-rippled sequence formed over the intervening neap-tide period. Due to the small width of the core, it is not precisely clear how many bundles were actually formed in each case, at least ten (representing 5 days) having been identified in the lower unit.

In contrast to the rather rare occurrence of tidal bundles in cross-bedded sand of back-barrier tidal flats, tidal bedding represented by sand-mud couplets is more frequently encountered. These are preferentially formed along mobile intertidal creeks as long as sufficient suspended matter is available to settle out at high tide. However, as intertidal creeks are rather shallow, one rarely finds more than just a few sand-mud couplets stacked above each other (Fig. 10.20). Each cycle begins on the rising tide as the tidal flat is inundated and the flood current begins to move sand across the sediment surface formed during the previous falling tide. Mud then settles out during the slack-water period over high tide and is subsequently covered by a sand layer in the course of the ebb tide. Each sand layer may be composed of two opposing current-generated ripple cross-stratified units, the thickness of each depending on the relative dominance of one current component over the other. In contrast to subtidal (de Boer et al. 1989) or intertidal estuarine rhythmites (Dalrymple et al. 1991), one would not expect large numbers of stacked couplets or any clear evidence of the daily inequality of the tide. At a larger spatial scale, a characteristic depositional facies is the so-called 'inclined heterolithic stratification' (Thomas et al. 1987). These form in the process of lateral channel migration or meandering, and are identified on the ground by what has also been called 'longitudinal' or 'lateral-accretion' bedding (Reineck 1958; Bridges and Leeder 1976).

As sand content decreases and mud content increases toward the mainland coast, the tidal flat gradually transforms into an almost featureless muddy plain, tidal channels or creeks being now restricted to locations where freshwater streams drain the hinterland. This is in stark contrast to non-barred macrotidal mud flats that are commonly sculptured into meandering

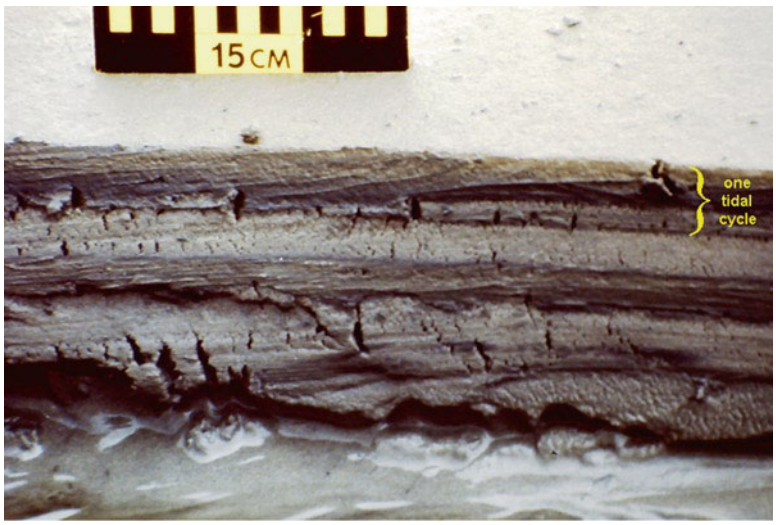

Fig. 10.20 Tidal bedding in form of vertically stacked mud-sand couplets along laterally migrating intertidal creeks. The mud settles out at high tide and is subsequently covered by a sand layer during the following ebb tide

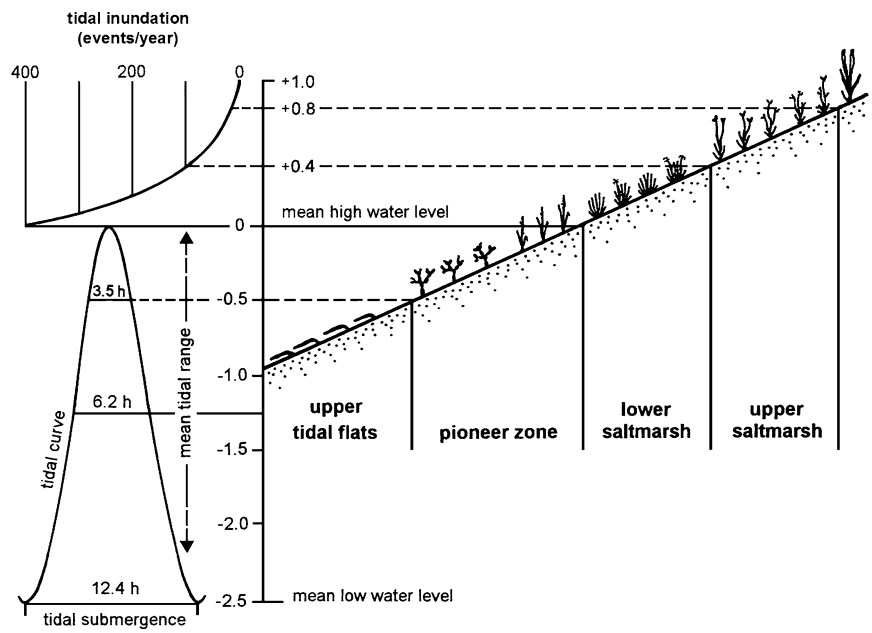

Fig. 10.21 Plant zonation pattern marking the transition from tidal flat to salt marsh (Modified after Streif 1990). In the Wadden Sea, the pioneer zone, which is occupied by *Salicornia* sp. and *Spartina* sp., begins at the elevation where the duration of tidal submergence is <3.5 h and terminates at the mean high-tide level where the salt marsh proper begins. Note that salt marsh zonation is primarily controlled by the annual frequency of inundation by seawater

tidal creeks and/or longitudinal mud ridges separated by erosional trenches (e.g., Gouleau et al. 2000; O'Brien et al. 2000). In back-barrier tidal basins, the monotonous muddy landscape only changes with the onset of vegetation, the uppermost tidal flats being colonized by so-called pioneer plants comprising halophytes (e.g., *Salicornia* and *Spartina*) which occupy a zone between the elevation where tidal submergence is <3.5 h (approx. 0.5 m below MHT in upper mesotidal settings) and the mean high-water line (Fig. 10.21).

The salt marsh proper begins at the mean high-water line, the transition between the halophytes of the pioneer zone and the salt resistant plants of the salt marsh being exceptionally sharp. The salt marsh itself

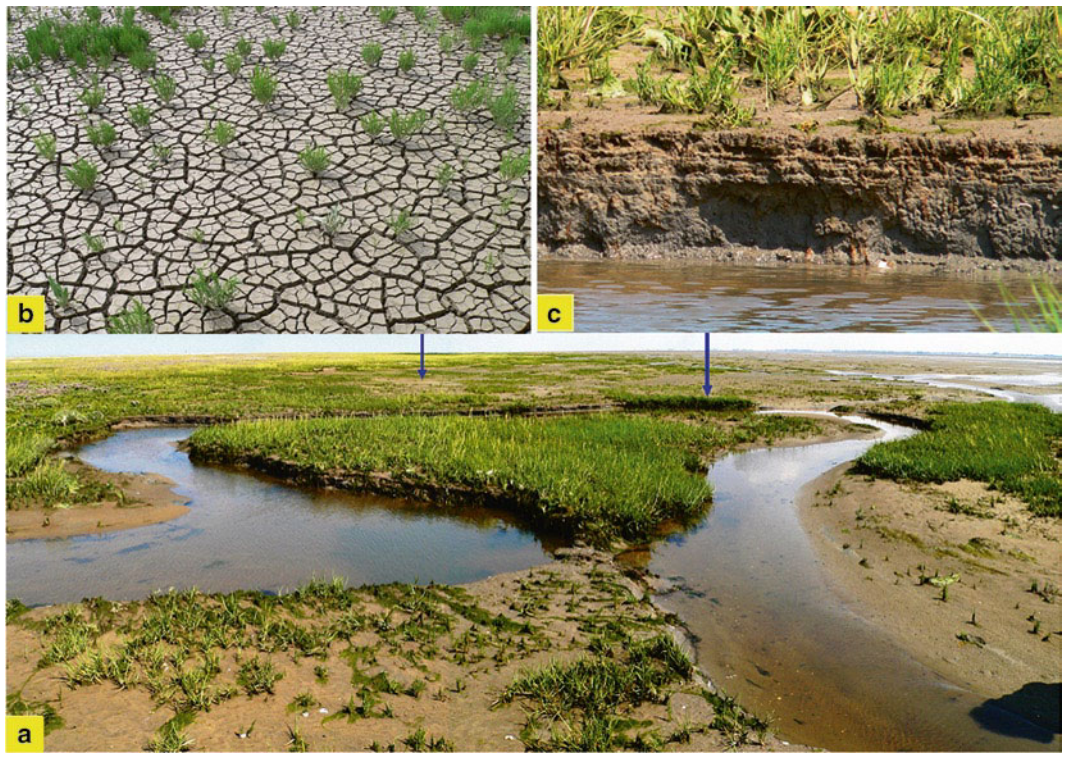

Fig. 10.22 Characteristic sedimentary features around the mean high-tide level. (**a**) Final meander of a salt marsh creek at low tide before draining onto the upper intertidal flat. Note that the water in the creek is not completely drained because it is dammed by a small 'ebb-delta' lobe at the transition to the open tidal flat; (**b**) Well developed mud cracks in sparsely vegetated *Salicornia* marsh; (**c**) Cut meander bank in *Spartina* marsh revealing preserved laminae near the surface and complete obliteration of physical structures at depth

can be subdivided further by specific plant associations comprising different species in different climates and geographic locations. In contrast to the smooth intertidal mud flats, the salt marshes are drained by an intricate network of meandering marsh creeks (Fig. 10.22a). Although the creek beds are generally excavated to depths below the elevation of the adjacent mud flats, they rarely extend into the latter as they commonly terminate in small 'ebb-delta' lobes at the salt marsh boundary where the channel-confined flow spreads out onto the open tidal flat. These depositional lobes often prevent the marsh creeks from draining completely at low tide.

Mud-cracked surfaces are frequently regarded as good indicators of emergence in tidal environments (Klein 1977). This applies in particular to tidal flat depositional systems with large differences between the elevations of neap high tide and spring high tide. The larger this difference, the longer the period of emergence over neap tide and the more extensive the mud-cracked surfaces. In regions where this difference in elevation is small, for example in the Wadden Sea, such surfaces are narrow and patchy (Fig. 10.22b). Mud-cracks and the roots of salt marsh plants tend to destroy any lamination in the course of time, as can be seen in Fig. 10.22c where the lamination is still preserved in the upper few centimetres but completely obliterated below (cf. also Fig. 10.18j).

In addition to the characteristic salt marsh zones associated with specific plants, the transition from upper intertidal to lower supratidal flats is locally characterized by laminated sediments (mats) produced by microbial activity, especially in places where this transition is more sandy (Fig. 10.23). As pointed out earlier, these microbial mats have to be carefully distinguished from algal mats produced by green algae (Gerdes and Krumbein 1987). Microbial mats commence at the sediment surface with a thin filamentous

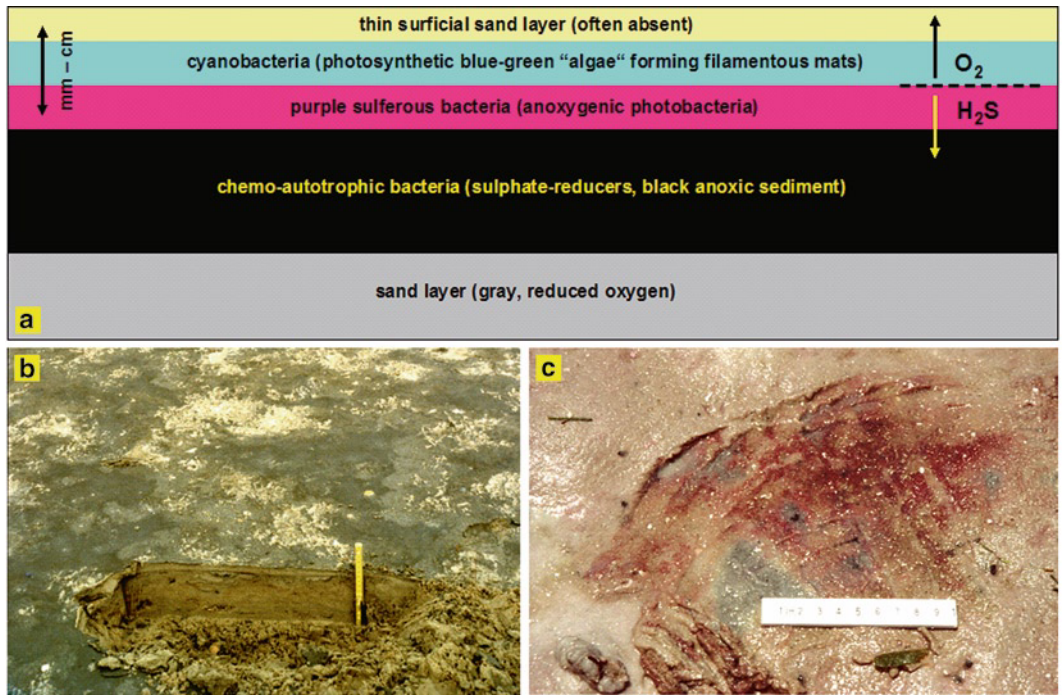

Fig. 10.23 Structure of a typical microbial mat occurring at the land-sea transition around the mean high-tide level (upper intertidal to lower supratidal). (**a**) Schematic model illustrating the vertical succession of bacteria in a typical microbial mat; (**b**) Photograph of a back-barrier microbial mat on the supratidal flat of a Wadden Sea island; (**c**) Intensely purple colored sulferous bacteria beneath a thin layer of sand in the rear of a Gulf Coast barrier island of Florida

carpet composed of oxygen-producing cyanobacteria (blue-green algae) (Fig. 10.23b). If covered by sand, the cyanobacteria migrate to the surface where a new mat is constructed, leaving behind the organic material of the old mat below the sand layer. The organic matter of the abandoned mat is then decomposed by so-called chemo-autotrophic sulphate-reducing bacteria in the course of which oxygen is depleted to produce a black anoxic layer. Just beneath the cyanobacterial mat anoxygenic sulferous photobacteria, identifiable by their intense purple color, are frequently observed. Being photobacteria, their activity increases markedly from the darker high latitudes towards the brighter low latitudes. Because of this, they are sometimes hard to spot in places like the Wadden Sea (55°N), whereas they occur in profusion in places like Florida (28°N) (Fig. 10.23c, cf. Davis 1994b). Because sand covering and subsequent upward migration of cyanobacteria occurs relatively frequently, several black horizons may be stacked above each other, the depletion of oxygen also affecting the sand below the mats which takes on a dark gray color. Due to the varied color scheme of the mats, this laminated microbial facies straddling the land-sea boundary has been given the apt name 'versicolored' tidal flat (Gerdes et al. 1985). When preserved, the characteristic lamination associated with specific bacteria makes it an excellent diagnostic tool for the identification of the land-sea boundary in the rock record (Schieber 2004; Noffke et al. 2006).

The trends of major parameters characterizing intertidal flats along the energy gradient between the mean low-tide and mean high-tide levels are summarized in Fig. 10.24. Parameters that decrease toward mean high tide include hydrodynamic energy, duration of water cover, submergence time, sand content of the sediment, and physical sediment reworking. The opposite trend is observed for mud content, exposure time, organic matter content, phytobenthos (diatoms), and plant fragments. Notable exceptions are seaweeds which preferentially occur on mixed flats, microbial mats that are restricted to a narrow zone around mean high tide, and last but not least the mass concentration

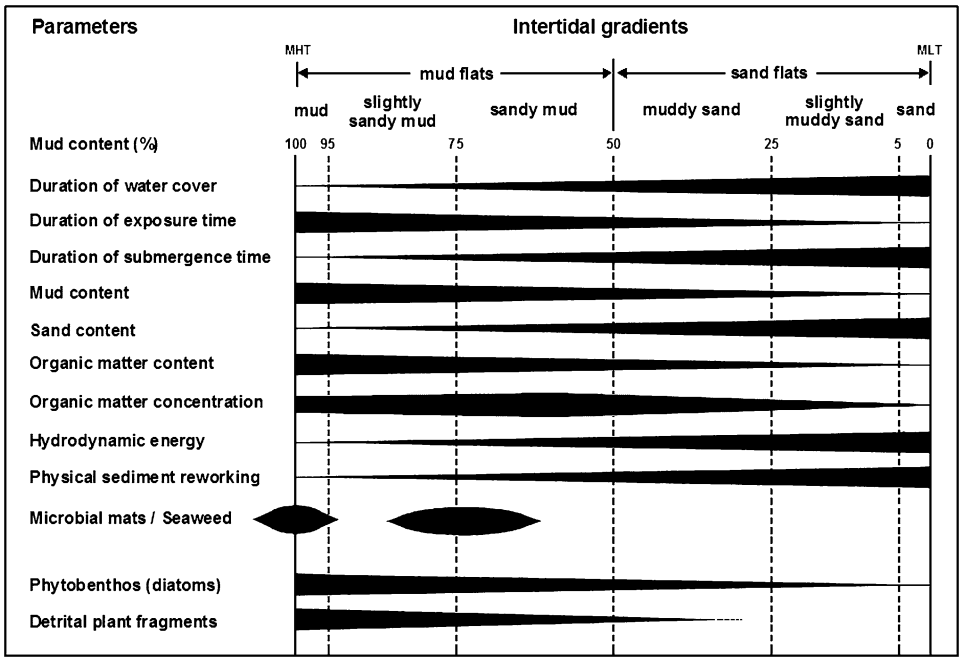

Fig. 10.24 Diagram summarizing the trends of major parameters characterizing intertidal flats. While most parameters either increase or decrease along the gradient between mean low tide (*MLT*) and mean high tide (*MHT*), the concentration (mass per unit volume) of organic matter peaks in the sandy mud facies, as would any other substance linked to the mud fraction (Modified after Hertweck 1994)

(mass per unit volume) of mud and any substances linked to the mud fraction. As outlined earlier, this would, for example, not only apply to the concentration of mud itself, but also to organic matter, heavy metals, trace elements, organic pollutants and toxic substances.

10.5 Stratigraphic Relationships

Having discussed and illustrated a variety of typical intertidal sedimentary structures and bedding types, the question arises of how these might be preserved in the rock record. Applying Walther's Law by vertically stacking typical sedimentary facies characterizing the intertidal gradient, a synthetic upward-coarsening transgressive facies model has been constructed (Fig. 10.25). The model is based on Reineck and Wunderlich (1968) and includes the most characteristic sedimentary structures generally observed along the intertidal gradient from sand flats near MLT to mud flats near MHT. While highlighting the most important primary sedimentary structures (flaser, wavy and lenticular bedding), the model is inherently incomplete because bioturbation, shell accumulations and sedimentary structures typical of intertidal creeks have been excluded. As such it would be more applicable to Precambrian than Phanerozoic tidal flats. However, as shown below, it serves a very useful purpose in that it simplifies the interpretation of generally much more complicated real-world situations.

Such a real-world situation, in this case representing a particular location in the modern Wadden Sea, is illustrated in Fig. 10.26 (after Chang et al. 2006c). The upward-coarsening sedimentary sequence recorded in the core clearly documents a transgressive setting commencing with mudflat deposits at the bottom and ending with sand flat deposits at the top. A closer look at the sequence reveals a number of features that complicate the interpretation. Thus, while the mudflat deposit in the lower core section is interspersed with thin lenticular beds as one would expect, the sequence does not progressively grade upward into wavy and lenticular bedding as required by the idealized model, but is

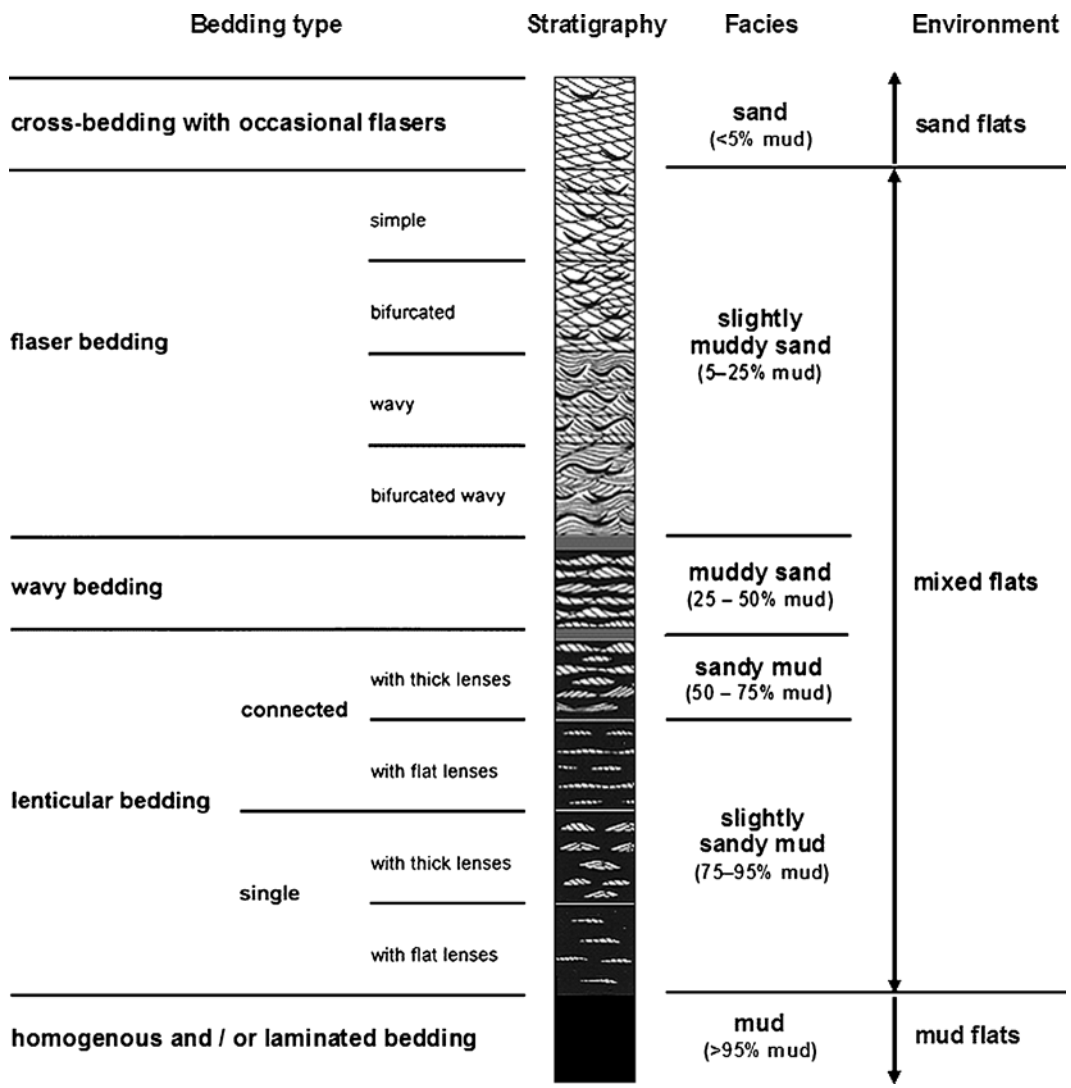

Fig. 10.25 Synthetic section in which successive sedimentary facies occurring between the low-tide and the high-tide level of intertidal flats (without tidal creeks and bioturbation) have been vertically stacked in an idealized transgressive facies model (Modified after Reineck and Wunderlich 1968; cf. also Flemming 2003a)

instead truncated by an erosional surface that is followed by an 80-cm thick sequence of alternating sand and shell beds, the latter being partly graded inversely. In the course of transgression and accretion, the former mudflat at the core site was evidently crossed a number of times by a migrating intertidal creek that reworked and destroyed any lenticular and wavy bedding that may have existed, leaving behind the reworked sand and shells in the form of stacked lag deposits. Above the channel deposits, the sequence continues with sparsely interspersed flaser beds and more prominently displayed cross-bedded sand of mostly wave-generated origin, alternating with thin mud layers typical of muddy and slightly muddy sand flats. Toward the top, the sequence grades into exposed sand flats. Significantly, bioturbation is only preserved in the uppermost layer.

As outlined above, the depositional sequence preserved in the core can be rationally explained on the basis of the idealized model, part of the expected

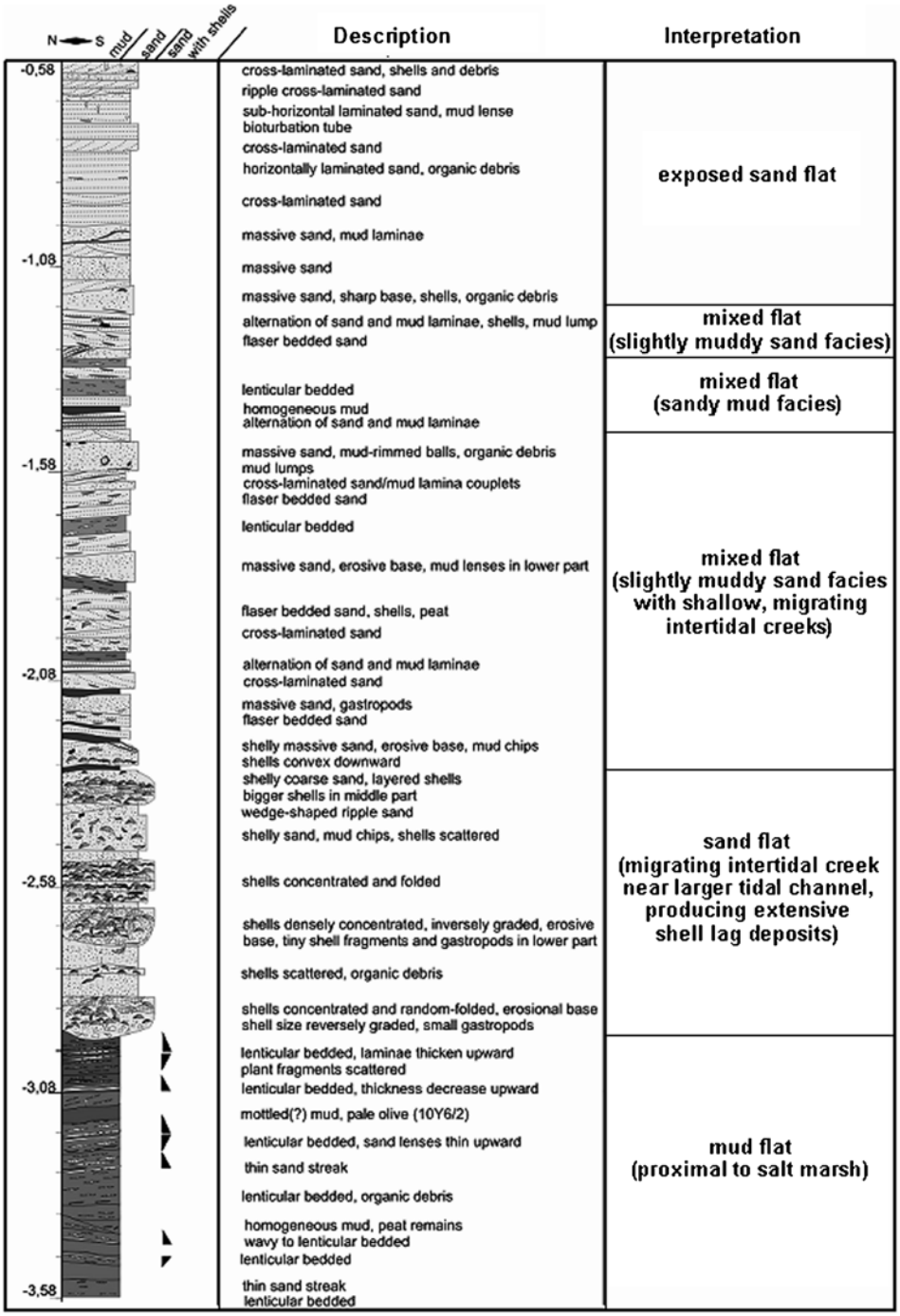

Fig. 10.26 Real-world transgressive section as observed in a vibro-core from the Wadden Sea (Modified after Chang et al. 2006c). Note the discontinuous nature of the succession and the multiple erosion surfaces

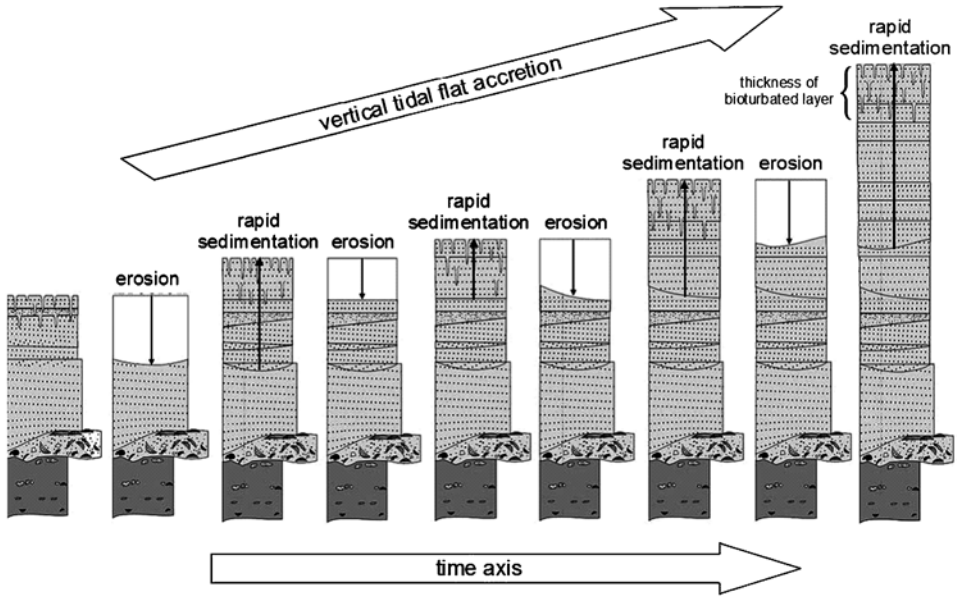

Fig. 10.27 Conceptual model illustrating the situation where physical reworking of the sediment outpaces bioturbation in the course of vertical accretion as observed in many parts of the Wadden Sea (Modified after Chang et al. 2006c)

sequence having simply been removed by migrating channels. Tidal-flat deposition above the channel sequence commences at higher energy conditions than required for the formation and preservation of lenticular, wavy and flaser bedding. The core demonstrates that, in the course of transgression, local conditions on a tidal flat can vary strongly, frequent depositional and erosional events ultimately resulting in only partial preservation of the potential record (Reineck 1960; van der Spek 1996). This not only concerns the preservation of particular sedimentary sequences as illustrated in the idealized model, but also the preservation of biological activity as suggested by the general absence of bioturbation throughout the core, except for the uppermost active layer. Within certain limits, the degree of preserved bioturbation is evidently an excellent criterion for the depth of reworking of a tidal flat by waves and/or currents. Because physical reworking of intertidal flats is generally restricted to the depth of intertidal creeks (~50 cm), this concept can only be applied to regions where the bioturbated layer is relatively thin (20–30 cm). This is generally the case in temperate climates. In subtropical and tropical climates, by contrast, callianassid shrimps will completely bioturbate the sediment to depths exceeding 1 m and hence obliterate the effects of physical reworking. Identification of the type of bioturbating organism(s) is thus a crucial prerequisite for the application of this concept to the rock record (Dott 1983, 1988).

For the temperate Wadden Sea, van Straaten (1954) presented a conceptual model that considers a number of different situations ranging from complete bioturbation to almost no bioturbation. The model was later modified slightly by Reineck and Singh (1980). As remarked earlier, only the uppermost 15 cm of the core in Fig. 10.26, i.e. the biologically active layer at the time of coring, is preserved. This means that the frequency and depth of reworking at the coring site has consistently outpaced bioturbation from the very start and thereby documents the rather exposed nature of the Wadden Sea (cf. Davis and Flemming 1995). This situation is illustrated in the conceptual model of Fig. 10.27 (after Chang et al. 2006c; cf. also van der Spek 1996).

As shown above, the succession of depositional facies along the intertidal gradient and their characteristic sedimentary structures will produce typical and easily recognized stratigraphic sequences in the course of vertical accretion. The main driving forces on geological time scales are changes in relative sea level and sediment supply, both being primarily controlled by

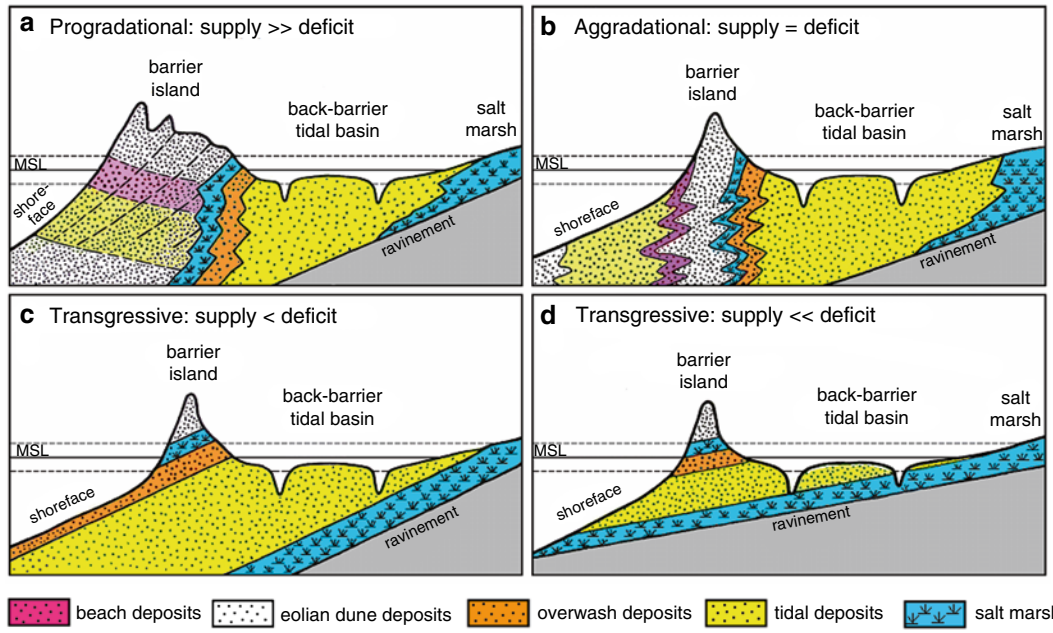

Fig. 10.28 Four geological cross-sections of barrier island depositional systems reflecting the stratigraphy produced by particular sediment budget situations controlled by the interaction betwen relative sea-level rise and sediment supply (Modified after Flemming 2002). Note that the shoreward fining sedimentary facies succession characterising the back-barrier tidal flat deposits (*yellow*) are not shown. Legend to color scheme includes beach, eolian dune, overwash, tidal flat (with channels), is salt marsh facies, but excludes the upper and lower shoreface

tectonic, isostatic and climatic processes acting either together or independently of each other. The interaction between the rate of relative sea-level rise and the rate of sediment supply defines the stratigraphic response of the system. Because sea-level fall leaves barrier islands and back-barrier tidal flats stranded, sustained accretion is usually associated with sea-level rise. In this context three basic stratigraphic response types can be distinguished, namely progradational, aggradational and retrogradational ones. Each has a characteristic and hence diagnostic stratigraphic expression (Galloway and Hobday 1975). The former two occasionally act in conjunction to produce aggrading progradational systems. In the case of both prograding and aggrading tidal flats, the entire depositional sequence is conserved (total retention), while in the retrogradational (transgressive) case varying parts of the sequence are lost, depending on the overall sediment deficit. For this reason it is useful to distinguish between partly conserved systems in which the depositional sequence is partially retained, and totally reworked systems in which only the final high-stand sequence is retained (Kraft 1971).

The main four types of stratigraphic responses outlined above are illustrated in the schematic cross-sections of Fig. 10.28. Each type represents a particular sediment budget situation that reflects the stratigraphic response resulting from the rate of sediment supply from external sources relative to the deficit created by sea-level rise over the same time interval. When keeping one of the control parameters constant, a change in the other will automatically affect the sediment budget, as a consequence of which the stratigraphic response changes from one state to another. It should be noted, however, that the four examples presented here represent time slices of particular sediment budget situations and that, in nature, one may find transitional systems reflecting budgets intermediate between any two of these. Furthermore, in the course of time, the sediment budget of a particular locality may change and an existing depositional type will then grade into another.

Cases a and b in Fig. 10.28 reflect the prograding and aggrading stratigraphies that result from a positive sediment budget where as much or more sediment is imported from external sources than required for the

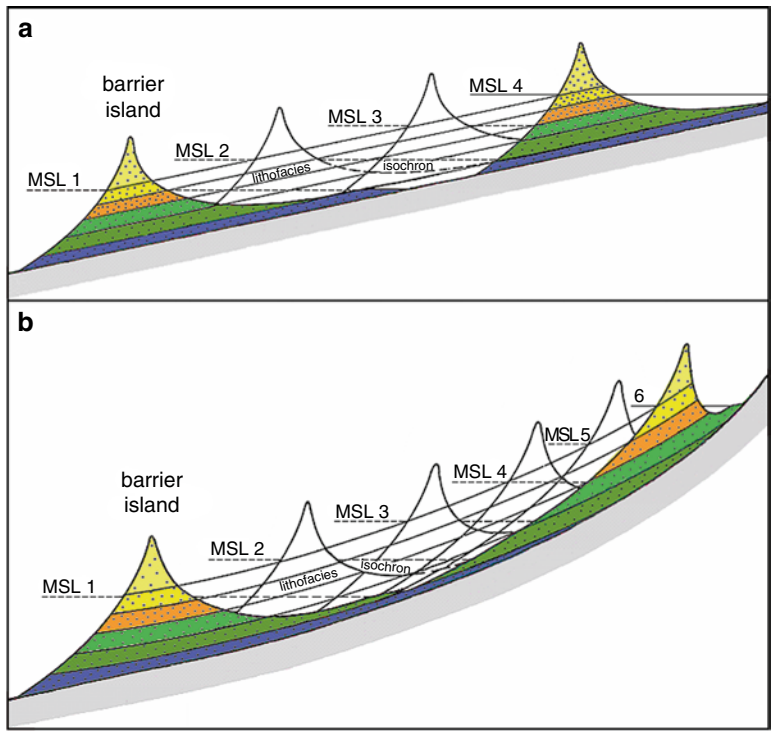

Fig. 10.29 Schematic conceptual models illustrating the stratigraphic situation in the case of a uniformly sloping (**a**) and a progressively steepening (**b**) shore. Note the squeezing out of individual sedimentary facies on the landward side in the latter case (Modified after Flemming and Bartholomä 1997)

compensation of the deficit created by sea-level rise. The difference between Figs. 10.28a, b mainly concerns the stratigraphy below the barrier island and the shoreface, the vertically aggrading back-barrier tidal flat systems (yellow colour) being more or less identical. As outlined earlier, the back-barrier deposits can also be identified by their progressive shoreward fining grain-size gradient which is not shown in Fig. 10.28. If less sediment is supplied from external sources than required to compensate sea-level rise, then the remaining deficit must be replaced by sediment from the existing reservoir. This involves moving sediment from the beach and upper shoreface toward the back-barrier basin. As a consequence, the barrier island is forced to migrate landward across its own back-barrier tidal flat. In the case where the remaining deficit is small, most of the depositional sequence is retained, the loss in the stratigraphic section being restricted to upper shoreface, beach, and barrier sands (Fig. 10.28c). The less sediment is available from external sources, the larger the remaining deficit and the fewer the depositional sequences retained in the stratigraphic section. At the same time the speed of barrier island migration increases. This may evolve to the point where no sediment is available from external sources and the deficit now has to be replaced entirely from the existing sediment reservoir (Fig. 10.28d). In this case the whole depositional sequence is progressively lost and only the final highstand deposit is retained for potential preservation in the rock record. The marked difference in depositional architecture produced by the variable interplay between sediment supply and sea-level rise thus turns out to be a powerful diagnostic tool for the interpretation of the stratigraphic record in terms of the temporal sediment budget evolution and the rate of sea-level change.

Thus far, the retention or loss of back-barrier deposits in the course of sea-level rise has been considered only in terms of changes in the sediment budget. In such cases, the progressive loss of sedimentary facies occurs on the seaward side, the capping barrier sand being eliminated first, the basal salt marsh last (Fig. 10.29a). This model applies to situations where a transgressive barrier-island depositional system

encroaches upon a low-lying coastal plain along a uniformly sloping surface. A reverse situation, or rather the simultaneous loss of sedimentary facies at both ends, appears to occur where a barrier system migrates up against a coastal cliff or a progressively steepening shore. Such a loss of finer-grained sedimentary facies along the mainland coast of the Wadden Sea was first recognised by Flemming and Nyandwi (1994). It was suggested to reflect the response of the back-barrier basin to land reclamation, the hydrodynamic energy – especially wave action – having increased as the water depth at high tide increased along the foot of the dike. This interpretation subsequently received strong support from a study in which the loss of accommodation space and the grain-size composition of tidal flats lost to land reclamation was numerically reconstructed (Mai and Bartholomä 2000). Thus, contrary to intuition, the widths of individual sedimentary facies belts do not simply adjust to fit into the reduced space, but the finer-grained ones are instead progressively eliminated.

A similar effect is postulated to occur along cliffed coasts or where a steepening slope obstructs normal barrier evolution, the latter case being illustrated in Fig. 10.29b. The process can be conceived to continue until the entire back-barrier depositional system has been removed and the former barrier sand has evolved into a perched coastal dune (Roy et al. 1994). This aspect in the stratigraphic evolution of barrier-island depositional systems has received little attention thus far. Nevertheless, some evidence favouring such an interpretation, even though not entirely conclusive, can be found in the literature (Curray et al. 1969; Belknap and Kraft 1977; Kraft et al. 1979. Vos and van Kesteren 2000).

10.6 Modern Examples and Ancient Analogues

10.6.1 Modern Examples

As pointed out earlier, most larger-scale back-barrier depositional systems documented in the literature lack substantial bare tidal flats, being instead dominated by salt marshes or mangroves and estuarine or lagoonal water bodies. As a consequence, there are few documented examples of modern bare siliciclastic back-barrier tidal flats that can match the Wadden Sea in scale and studied detail (Klein 1976). Excellent regional summaries covering various aspects of Wadden Sea research, including comprehensive literature citations up to the time of publication, can be found in Reineck and Singh (1980), Dijkema et al. (1980), Postma (1982), Ehlers (1988), Oost and de Boer (1994), Flemming and Davis (1994), Flemming and Hertweck (1994), and Bartholdy and Pejrup (1994).

Among back-barrier tidal flat systems that merit being mentioned here are the ones off the Copper River delta located along the Pacific coast of Alaska (Reimnitz 1966; Galloway 1976; Hayes and Ruby 1994). However, little detail on intertidal sediment distribution and sedimentary structures has been published. The same, in principle, holds for the enigmatic Ria Formosa (Algarve) barrier island system off southern Portugal, which is unique in the sense that it is a non-coastal plain system backed by a steeply rising coastal cliff. The accessible literature (Pilkey et al. 1989; Davis 1994a) mostly concentrates on the barrier islands and provides little information on the back-barrier tidal flats. Some geomorphological, sedimentological and geochemical data exist but are difficult to access (Granja 1984; Granja et al. 1984; Monteiro et al. 1984; Dias 1986). Because the barrier island chain gradually approaches the coastal cliff towards the border of Spain, it could represent an ideal case to validate the concept of progressive loss of finer-grained sediment facies along the foot of the cliff as the back-barrier tidal flats get narrower.

The back-barrier systems along the east and south coasts of the North American continent are mostly of the lagoonal and/or estuarine type with extensive salt marshes covering the intertidally exposed parts with no or only very narrow bare intertidal flats. These locally display stratigraphies that are similar to more extensive tidal flat systems such as the Wadden Sea. Examples can be found in Leatherman (1979), FitzGerald et al. (1994), Hayes (1994) and Oertel and Kraft (1994).

A variety of back-barrier tidal flat system that does not quite correspond to the classic type discussed here, are coastal lagoons in which intertidal flats occupy a large part of the area. Well documented examples of this type are Willapa Bay along the Pacific coast of the USA (Clifton et al. 1989; Dingler and Clifton 1994) and Langebaan Lagoon along the west coast of South Africa (Flemming 1977). The main difference to classic back-barrier tidal flats is the fact that the grain-size

gradient (and hence the energy gradient) is not perpendicular to the coast, but instead more or less aligned along the main axis of the lagoon between the mouth and the head. Other than this, the intertidal flats display many of the features discussed in this contribution.

10.6.2 Ancient Analogues

Examples of tidal deposits span the time period from the Early Archaean to the present (Noffke et al. 2006; Noffke 2010) and it would go beyond the scope of this contribution to cite them all. This section therefore restricts itself to a listing of important collective works that deal with clastic tidal deposits and which also include ancient examples. A first symposium proceedings specifically dedicated to tidal research was edited by Ginsburg (1975). Hobday and Errikson (1977) present the results of a tidal conference with special reference to South African case studies. An exhaustive summary of both modern and ancient examples up to the year 1977 can be found in Klein (1977). Other conference proceedings containing case studies from modern and ancient tidal environments include de Boer et al. (1988), Smith et al. (1991), Flemming and Bartholomä (1995), Alexander et al. (1998), Park and Davis (2001), and Bartholdy and Kvale (2006).

The cited works demonstrate that tidal-flat deposits can generally be recognized in the rock record with some degree of confidence. However, it is much more difficult, and in many cases impossible, to differentiate between micro-mesotidal back-barrier tidal flats and macrotidal open coast counterparts. Both display essentially the same range of surface features and internal sedimentary structures. Being more energetic, macrotidal flats should display a greater proportion of larger-scale dune cross-bedding relative to smaller-scale ripple cross-bedding on sand flats than would be the case on mesotidal flats where dune cross-bedding is the exception rather than the rule. Another feature that is more prominent on macrotidal flats is the occurrence of relatively high (>1 m) intertidal bars entirely composed of bioclastic material (mollusc shells) that may be found up to and even within salt marsh deposits (e.g., Larsonneur 1994; Schneider-Storz et al. 2008).

As the features addressed above are not unequivocally diagnostic, in addition to requiring excellent outcrop conditions, some researchers have looked for ways to estimate paleotidal ranges in order to solve this problem (Klein 1971; Allen 1981; Terwindt 1988). In each case, a different approach was used. Thus, Klein (1971) suggested that the thickness of upward-fining sequences approximated the paleotidal range, whereas Allen (1981) used the thickness of cross-bedding sets displaying mud drapes to derive at such estimates. Terwindt (1988), in turn, used a complex combination of stratigraphic criteria to reconstruct paleotidal ranges, but submits that this was very difficult because reliable criteria to identify the low-water line were lacking. Although very persuasive, this issue has not really been resolved to this day.

An elegant way to decide whether a tidal deposit was formed in a back-barrier setting would be the identification of the ancient barrier itself, or at least remnants thereof, in the rock record. Criteria for this have been summarized by Dickinson et al. (1972). This would side-step the issue of having to estimate paleotidal range, but would again require good exposures in the field. Finally, tidal euphoria can also lead to astonishing misinterpretations. Thus, the supposedly 'transgressive-barrier and shallow shelf interpretation of the lower Paleozoic Peninsula Formation, South Africa' (Hobday and Tankard 1978) is more likely a large alluvial fan delta that incorporates a few thin marine transgressions (Brian Turner, personal communication 1993). The interpretation can be shown to have been based on non-conclusive evidence and that other features such as the occurrence of massive pebble beds, ubiquitous floating pebbles, stacked linguoid bars, sand-draped mud cracks, and especially the total absence of any tidal rhythmites in any of the excellent exposures collectively favor an alluvial origin (Flemming, unpublished).

References

Alexander CR, Davis RA, Henry VJ (eds) (1998) Tidalites: processes and products. SEPM Spec Publ 61

Allen JRL (1981) Palaeotidal speeds and ranges estimated from cross-bedding sets with mud drapes. Nature 293:394–396

Allen PA, Homewood P (1984) Evolution and mechanics of a Miocene tidal sandwave. Sedimentology 31:63–81

Anderson FE (1983) The northern muddy intertidal: seasonal factors controlling erosion and deposition – a review. Can J Fish Aquat Sci 40:143–159

Arends F (1833) Physische Geschichte der Nordsee-Küste und deren Veränderungen durch Sturmfluthen seit der Cymbrischen Fluth bis jetzt. Woortmann, Emden, vol 1,

384 pp; vol 2, 355 pp. Facsimile reprinting in one volume 1974. Verlag Schuster, Leer

Ashley GM (1988) The hydrodynamics and sedimentology of a back-barrier lagoon-salt marsh system, Great Sound, New Jersey. Mar Geol 82:1–132

Aubrey DG, Speer PE (1985) A study of non-linear tidal propagation in shallow inlet/estuarine systems, Part I: observations. Estuar Coast Shelf Sci 21:185–205

Bartholdy J, Kvale EP (eds) (2006) Proceedings of the 6th international congress on tidal sedimentology (Tidalites 2004), 02–05 Aug 2004, Copenhagen. Mar Geol 235, 272 pp

Bartholdy J, Pejrup M (1994) Holocene evolution of the Danish Wadden Sea. In: Flemming BW, Hertweck G (eds) Tidal flats and barrier systems of continental Europe: a selected overview. Senckenberg marit 24:187–209

Bartholomä A, Flemming BW (2007) Progressive grain-size sorting along an intertidal energy gradient. Sed Geol 202:464–472

Bartholomä A, Flemming BW, Delafontaine MT (2000) Mass balancing the seasonal turnover of mud and sand in the vicinity of an intertidal mussel bank in the Wadden Sea (southern North Sea). In: Flemming BW, Delafontaine MT, Liebezeit G (eds) Muddy coast dynamics and resource management. Elsevier Science, Amsterdam, pp 85–106

Beets DJ, Fischer MM, de Gans W (eds) (1996) Coastal studies on the Holocene of the Netherlands. Mededel Rijks Geologische Dienst 57

Belknap DF, Kraft JC (1977) Holocene relative sea-level changes and coastal stratigraphic units on the northwest flank of the Baltimore Canyon trough geosyncline. J Sed Petrol 47:610–629

Biegel E, Hoekstra P (1995) Morphological response characteristics of the Zoutkamperlaag, Frisian inlet (The Netherlands), to a sudden reduction in basin area. In: Flemming BW, Bartholomä A (eds) Tidal signatures in modern and ancient sediments. Int Assoc Sediment Spec Publ 24:85–99

Boon JD III, Byrne RJ (1981) On basin hypsometry and the morphodynamic response of coastal inlet systems. Mar Geol 40:27–48

Boothroyd JC, Friedrich NE, McGinn SR (1985) Geology of microtidal coastal lagoons, Rhode Island. Mar Geol 63:35–76

Bouma AH (1969) Methods for the study of sedimentary structures. Wiley-Interscience, New York

Bridges PH, Leeder MR (1976) Sedimentary model for intertidal mudflat channels, with examples from the Solway Firth, Scotland. Sedimentology 23:533–552

Burchard H, Flöser G, Staneva JV, Badewien T, Riethmüller R (2008) Impact of density gradients on net sediment transport into the Wadden Sea. J Phys Oceanog 38:566–587

Carver RE (ed) (1971) Procedures in sedimentary petrology. Wiley-Interscience, New York

Chang TS, Flemming BW (2006) Sedimentation on a wave-dominated, open-coast tidal flat, southwestern Korea: summer tidal flat–winter shoreface – discussion. Sedimentology 53:687–691

Chang TS, Bartholomä A, Flemming BW (2006a) Seasonal dynamics of fine-grained sediments in a back-barrier tidal basin of the German Wadden Sea (southern North Sea). J Coast Res 22:328–338

Chang TS, Joerdel O, Flemming BW, Bartholomä A (2006b) Importance of flocs and aggregates in muddy sediment dynamics and seasonal sediment turnover in a back-barrier tidal basin of the East Frisian Wadden Sea (southern North Sea). Mar Geol 235:49–61

Chang TS, Flemming BW, Tilch E, Bartholomä A, Wöstmann R (2006c) Late Holocene stratigraphic evolution of a back-barrier tidal basin in the East Frisian Wadden Sea, southern North Sea: transgressive deposition and its preservation potential. Facies 52:329–340

Chang TS, Flemming BW, Bartholomä A (2007) Distinction between sortable silts and aggregated particles in muddy intertidal sediments of the southern North Sea. In: Flemming BW, Hartmann D (eds) From particle size to sediment dynamics. Proceeding of a workshop, Hanse Instituite for Advanced Study, Delmenhorst (Germany), 15–18 Apr 2004. Sed Geol 202:453–463

Clifton HE, Phillips RL, Anima RJ (1989) Sedimentary facies of Willapa Bay, Washington; a field guide. Can Soc Petrol Geol Mem 16

Curray JR, Emmel FJ, Crampton PJS (1969) Holocene history of a strand plain, lagoonal coast, Nayarit, Mexico. In: Castanares AA, Phleger FB (eds) Coastal lagoons – a symposium. Universidad Autonoma, Mexico City, pp 63–100

Dalrymple RW, Makino Y, Zaitlin BA (1991) Temporal and spatial patterns of rhythmite deposition on mudflats in the macrotidal, Cobequid Bay-Salmon River estuary, Bay of Fundy, Canada. In: Smith DG, Reinson GE, Zaitlin BA, Rahmani RA (eds) Clastic tidal sedimentology. Can Soc Petrol Geol Mem 16:137–160

Dalrymple RW, Zaitlin BA, Boyd R (1992) Estuarine facies models: conceptual basis and stratigraphic implications. J Sed Petrol 62:1130–1146

Dastgheib A, Roelvink JA, Wang ZB (2008) Long-term process-based morphological modeling of the Marsdiep tidal basin. Mar Geol 256:90–100

Davies JL (1964) A morphogenetic approach to the world shorelines. Zeitschr f Geomorph 8:127–142

Davis RA Jr (ed) (1994a) Geology of Holocene barrier island systems. Springer, Berlin

Davis RA Jr (1994b) Barriers of the Florida Peninsula. In: Davis RA Jr (ed) Geology of Holocene barrier island systems. Springer, Berlin, pp 167–205

Davis RA Jr, Flemming BW (1995) Stratigraphy of a combined wave- and tide-dominated intertidal sand body: Martens Plate, German Wadden Sea. In: Flemming BW, Bartholomä A (eds) Tidal signatures in modern and ancient sediments. Spec Publ Int Assoc Sediment 24:121–132

Davis RA Jr, Hayes MO (1984) What is a wave-dominated coast? Mar Geol 60:313–329

de Bèaumont LE (1845) Septième Leçon: Léeves de sable et de galet. In: Bertrand P (ed) Leçons de géologie practique. Masson, Paris, pp 221–252

de Boer PL (1979) Convolute lamination in modern sands of the estuary of the Oosterschelde, the Netherlands, formed as a result of entrapped air. Sedimentology 26:283–294

de Boer PL, van Gelder A, Nio SD (eds) (1988) Tide-influenced sedimentary environments and facies. D Reidel Publishing Company, Dordrecht

de Boer PL, Oost AP, Visser MJ (1989) The diurnal inequality of the tide as a parameter for recognizing tidal influences. J Sed Petrol 59:912–921

de Raaf JFM, Boersma JR (1971) Tidal deposits and their sedimentary structures (seven examples from Western Europe). Geol Mijn 50:479–504

Delafontaine MT, Flemming BW, Bartholomä A (2000) Mass balancing the seasonal turnover of POC in mud and sand on a back-barrier tidal flat (southern North Sea). In: Flemming BW, Delafontaine MT, Liebezeit G (eds) Muddy coast dynamics and resource management. Elsevier Science, Amsterdam, pp 107–124

Delafontaine MT, Flemming BW, Thimm M (2004) Large-scale trends in some mass physical properties of Danish Wadden Sea sediments, and implications for organism-sediment interactions. Danish J Geog 104:27–36

Dias JMA (1986) Observacoes sobre a origem das areias das ilhas barreira da Ria Formosa. 4th Congr Algarve. Textos das Comunicaçoes 1:579–587

Dickinson KA, Berryhill HL Jr, Holmes CW (1972) Criteria for recognizing ancient barrier coastlines. In: Rigby JK, Hamblin WK (eds) Recognition of ancient sedimentary environments. SEPM Spec Publ 16:192–204

Dijkema KS, Reineck H-E, Wolff WJ (eds) (1980) Geomorphology of the Wadden Sea area. In: Wadden Sea Working Group (eds) Final report of the section 'Geomorphology'. AA Balkema, Rotterdam

Dingler JR, Clifton HE (1994) Barrier systems of California, Oregon, and Washington. In: Davis RA Jr (ed) Geology of Holocene barrier island systems. Springer, Berlin, pp 115–165

Dionne JC (1974) How drift ice shapes the St. Lawrence. Can Geogr J 88:4–9

Dionne JC (1988) Characteristic features of modern tidal flats in cold regions. In: de Boer PL, van Gelder A, Nio SD (eds) Tide-influenced sedimentary environments and facies. D Reidel Publishing Company, Dordrecht, pp 301–332

Dissanayake DMPK, van der Roelvink JA, Wegen M (2009) Modelled channel patterns in a schematized tidal inlet. Coast Eng 56:1069–1083

Dott RH Jr (1983) Episodic sedimentation – how normal is average? How rare is rare? Does it matter? J Sed Petrol 53:5–23

Dott RH Jr (1988) An episodic view of shallow marine clastic sedimentation. In: de Boer PL, van Gelder A, Nio SD (eds) Tide-influenced sedimentary environments and facies. D Reidel Publishing Company, Dordrecht, pp 3–12

Dronkers J (1986) Tidal asymmetry and estuarine morphology. Neth J Sea Res 20:107–131

Dunn IS, Anderson LR, Kiefer FW (1980) Fundamentals of geotechnical analysis. Wiley, New York

Ehlers J (1988) Morphodynamics of the Wadden Sea. AA Balkema, Rotterdam, 397 pp

Einsele G (1963) "Convolute bedding" und ähnliche Sedimentstrukturen im rheinischen Oberdevon und anderen Ablagerungen. N Jb Paläont, Abh 116:162–189

FitzGerald DM, Rosen PS, van Heteren S (1994) New England barriers. In: Davis RA Jr (ed) Geology of Holocene barrier island systems. Springer, Berlin, pp 305–394

Flemming BW (1977) Langebaan Lagoon: a carbonate–siliciclastic tidal environment in a semi-arid climate. Sed Geol 18:61–95

Flemming BW (2000) A revised textural classification of gravel-free muddy sediments on the basis of ternary diagrams. Cont Shelf Res 20:1125–1137

Flemming BW (2002) Effects of climate and human interventions on the evolution of the Wadden Sea depositional system (southern North Sea). In: Wefer G, Berger W, Behre KE, Jansen E (eds) Climate development and history of the North Atlantic Realm. Springer, Berlin, pp 399–413

Flemming BW (2003a) Flaser. In: Middleton GV (ed) Encyclopedia of sediments and sedimentary rocks. Kluwer, Dordrecht, pp 282–283

Flemming BW (2003b) Tidal flats. In: Middleton GV (ed) Encyclopedia of sediments and sedimentary rocks. Kluwer, Dordrecht, pp 734–737

Flemming BW (2005) Tidal environments. In: Schwartz M (ed) Encyclopedia of coastal science. Springer, Berlin, pp 1180–1185

Flemming BW (2007) The influence of grain-size analysis methods and sediment mixing on curve shapes and textural parameters: implications for sediment trend analysis. Sed Geol 202:425–435

Flemming BW, Bartholomä A (eds) (1995) Tidal signatures in modern and ancient sediments. Int Assoc Sed Spec Publ 24

Flemming BW, Bartholomä A (1997) Response of the Wadden Sea to a rising sea level: a predictive empirical model. Ger J Hydrogr 49:343–353

Flemming BW, Davis RA Jr (1994) Holocene evolution, morphodynamics and sedimentology of the Spiekeroog barrier island system (southern North Sea). In: Flemming BW, Hertweck G (eds) Tidal flats and barrier systems of continental Europe: a selected overview. Senckenberg marit 24:117–155

Flemming BW, Delafontaine MT (2000) Mass physical properties of intertidal muddy sediments: some applications, misapplications and non-applications. Cont Shelf Res 20:1179–1197

Flemming BW, Hertweck G (eds) (1994) Tidal flats and barrier systems of continental Europe: a selected overview. Senckenberg marit 24

Flemming BW, Nyandwi N (1994) Land reclamation as a cause of fine-grained sediment depletion in backbarrier tidal flats (southern North Sea). Neth J Aquat Ecol 28:299–307

Flemming BW, Ziegler K (1995) High-resolution grain size distribution patterns and textural trends in the backbarrier tidal flats of Spiekeroog Island (southern North Sea). Senckenberg marit 26:1–24

Folk RL (1954) The distinction between grain size and mineral composition in sedimentary-rock nomenclature. J Geol 62:344–359

Fortunato AB, Oliveira A (2004) A modelling system for tidally driven long-term morphodynamics. J Hydraul Res 42:426–434

Frey RW, Basan PB (1985) Coastal salt marshes. In: Davis RA Jr (ed) Coastal sedimentary environments, 2nd edn. Springer, New York, pp 225–301

Frey RW, Howard JD (1969) A profile of biogenic sedimentary structures in a Holocene barrier island salt marsh complex, Georgia. Trans Gulf Coast Assoc Geol Soc 19:427–444

Friedrichs CT, Aubrey DG (1988) Non-linear tidal distortion in shallow well-mixed estuaries: a synthesis. Estuar Coast Shelf Sci 27:521–545

Friedrichs CT, Lynch DR, Aubrey DG (1992) Velocity asymmetries in frictionally-dominated tidal embayments: longitudinal and lateral variability. In: Prandle D (ed) Dynamics and exchanges in estuaries and the coastal zone. American Geophysical Union, Washington, DC, pp 277–312

Galloway WE (1976) Sediments and stratigraphic framework of the Copper River fan delta. J Sed Petrol 46:726–737

Galloway WE, Hobday DK (1975) Terrigenous clastic depositional systems. Springer, Berlin, pp 234

Ganju NK, Schoellhamer DH, Jaffe BE (2009) Hindcasting of decadal-timescale estuarine bathymetric change with a tidal-timescale model. J Geophys Res 114:F04019. doi:10.1029/2008JF001191

Gerdes G, Krumbein WE (1987) Biolaminated deposits. Lecture notes in earth sciences 9. Springer, Berlin

Gerdes G, Krumbein WE, Reineck H-E (1985) The depositional record of sandy, versicolored tidal flats (Mellum Island, southern North Sea). J Sed Petrol 55:265–278

Ginsburg RN (ed) (1975) Tidal deposits – a casebook of recent examples and fossil counterparts. Springer, Berlin/Heidelberg/New York

Glaeser JD (1978) Global distribution of barrier islands in terms of tectonic setting. J Geol 86:283–297

Gouleau D, Jouanneau JM, Weber O, Sauriau PG (2000) Short- and long-term sedimentation on Montportail–Brouage intertidal mudflat, Marennes–Oléron Bay (France). Cont Shelf Res 20:1513–1530

Granja H (1984) Etude géomorphologique, sédimentologique et géochimique de la "Ria Formose" (Algarve-Portugal). Thése Zeme cycle, n 1944, Université de Bordeaux I, Bordeaux, France

Granja H, Froidefond J-M, Pera T (1984) Processus d'évolution morpho-sédimentaire de la Ria Formosa (Portugal). Bull Inst Géol Bassin d'Aquitaine 36:37–50

Groen P (1967) On the residual transport of suspended matter by an alternating tidal current. Neth J Sea Res 3:564574

Hack JT (1957) Studies of longitudinal stream profiles in Virginia and Maryland. US Geol Surv Prof Paper 219B

Haven DS, Morales-Alamo R (1968) Occurrence and transport of fecal pellets in suspension in a tidal estuary. Sed Geol 2:141–151

Hayes MO (1979) Barrier island morphology as a function of tidal and wave regime. In: Leatherman SP (ed) Barrier islands. Academic, New York, pp 1–27

Hayes MO (1994) The Georgia Bight barrier systems. In: Davis RA Jr (ed) Geology of Holocene barrier island systems. Springer, Berlin, pp 233–304

Hayes MO, Ruby CH (1994) Barriers of Pacific Alaska. In: Davis RA Jr (ed) Geology of Holocene barrier island systems. Springer, Berlin, pp 395–433

Hertweck G (1994) Zonation of benthos and lebensspuren in the tidal flats of the Jade Bay, southern North Sea. In: Flemming BW, Hertweck G (eds) Tidal flats and barrier systems of continental Europe: a selected overview. Senckenberg marit 24:157–170

Hillel D (1998) Environmental soil physics. Academic, San Diego

Hobday DK, Errikson KA (eds) (1977) Tidal sedimentation with special reference to South African examples. Sed Geol 18

Hobday DK, Tankard AJ (1978) Transgressive-barrier and shallow-shelf interpretation of the lower Paleozoic Peninsula Formation, South Africa. Geol Soc Am Bull 89:1733–1744

Howard JD, Frey RW (1975) Estuaries of the Georgia coast, U.S.A.: Sedimentology and Biology. II. Regional animal-sediment characteristics of Georgia estuaries. Senckenberg marit 7:33–103

Hume TM, Herdendorf CE (1992) Factors controlling tidal inlet characteristics on low drift coasts. J Coast Res 8:355–375

Inderbitzen AL (ed) (1974) Deep-sea sediments: physical and mechanical properties. Plenum, New York

Jakobsen B (1962) The formation of ebb and flood channels in tidal channels described on basis of morphological and hydrological observations. Geogr Tijdskrift 61:119–149

Jarrett JT (1976) Tidal prism-inlet area relationships. US Army Corps of Engineers, Coastal Engineering Research Center and Waterways Experimental Station, Vicksburg. GITI report 3

Jennings JN, Coventry RJ (1973) Structure and texture of a gravely barrier island in the Fitzroy estuary, Western Australia, and the role of mangroves in the shore dynamics. Mar Geol 15:145–167

Johnson DW (1919) Shore processes and shore line development. Wiley, New York, 584 pp

Kindle EM (1917) Recent and fossil ripple marks. Geol Surv Can Museum Bull 25

Kirby R (2000) Practical implications of tidal flat shape. Cont Shelf Res 20:1061–1077

Klein G (1971) A sedimentary model determining paleotidal range. Geol Soc Am Bull 82:2585–2592

Klein G (1977) Clastic tidal facies. CEPCO, Champaign

Klein G (ed) (1976) Holocene tidal sedimentation. Benchmark papers in geology 30. Dowden, Hutchinson & Ross, Stroudsburg

Kraft JC (1971) Sedimentary facies patterns and geologic history of a Holocene marine transgression. Geol Soc Am Bull 82:2131–2151

Kraft JC, Allen EA, Belknap DF, John CJ, Maurmeyer EM (1979) Processes and morphologic evolution of an estuarine and coastal barrier system. In: Leatherman SP (ed) Barrier islands – from the Gulf of St. Lawrence to the Gulf of Mexico. Academic, New York, pp 149–183

Krögel F, Flemming BW (1998) Evidence for temperature-adjusted sediment distributions in the backbarrier tidal flats of the East Frisian Wadden Sea (southern North Sea). In: Alexander CR, Davis RA, Henry VJ (eds) Tidalites: processes & products. SEPM, Tulsa, Spec Publ 61:31–41

Krone RB (1972) A field study of flocculation as a factor in estuarine shoaling processes. Committee on Tidal Hydraulics, US Army Corps of Engineers. Technical Bulletin 19

Lambe WT, Whitman RV (1969) Soil mechanics. Wiley, New York

Larsonneur C (1994) The bay of Mont–Saint–Michel: a sedimentation model in a temperate macrotidal environment. In: Flemming BW, Hertweck G (eds) Tidal flats and barrier systems of continental Europe: a selected overview. Senckenberg marit 24:3–63

Leatherman SP (ed) (1979) Barrier islands – from the Gulf of St. Lawrence to the Gulf of Mexico. Academic, New York

Leopold LB, Wolman MG, Miller JP (1964) Fluvial processes in geomorphology. Freeman, San Francisco

Lettmann KA, Wolff J-O, Badewien TH (2009) Modelling the impact of wind and waves on suspended particulate matter fluxes in the East Frisian Wadden Sea (southern North Sea). Ocean Dyn 59:239–262

Mai S, Bartholomä A (2000) The missing mud flats of the Wadden Sea: a reconstruction of sediments and accommodation space lost in the wake of land reclamation. In: Flemming BW, Delafontaine MT, Liebezeit G (eds) Muddy coast dynamics and resource management. Elsevier Science, Amsterdam, pp 257–272

McCave IN, Manighetti B, Robinson SG (1995) Sortable silt and fine sediment size/composition size slicing: parameters for palaeocurrent speed and palaeoceanography. Paleoceanography 10:593–610

Migniot C (1968) A study of the physical properties of various forms of very fine sediments and their behaviour under hydrodynamic action. La Houille Blanche 7:591–620

Miller JA (1975) Facies characteristics of Laguna Madre windtidal flats. In: Ginsburg RN (ed) Tidal deposits. Springer, New York, pp 67–72

Molinaroli E, Guerzoni S, De Falco G, Saretta A, Cucco A, Como S, Simeone S, Perilli A, Magni P (2009) Relationships between hydrodynamic parameters and grain size in two contrasting transitional environments: the Lagoons of Venice and Cabras, Italy. Sed Geol 219:196–207

Monteiro JH, Pilkey O, Dias JA, Gaspar LC, Paixo G (1984) Origem, evoluçao e processos geologicos das ilhas barreira a sua importancia para o desenvolvimento destas ilhas. 3 rd Congresso Sobre o Algarve. Textos das Comunicaçoes 2:713–719

Nichols MM, Biggs RB (1985) Estuaries. In: Davis RA Jr (ed) Coastal sedimentary environments. Springer, New York, pp 77–186

Noffke N (2010) Geobiology – microbial mats in sandy deposits from the Archaean Era to today. Springer, Heidelberg

Noffke N, Eriksson KA, Hazen RM, Simpson EL (2006) A new window into Early Archean life: microbial mats in Earth's oldest siliciclastic tidal deposits (3.2 Ga Moodies Group, South Africa). Geology 34:253–256

Nyandwi N, Flemming BW (1995) A hydraulic model for the shore-normal energy gradient in the East Frisian Wadden Sea (southern North Sea). Senckenberg marit 25:163–171

O'Brien DJ, Whitehouse RJS, Cramp A (2000) The cyclic development of a macrotidal mudflat on varying timescales. Cont Shelf Res 20:1593–1619

Oertel GF, Kraft JC (1994) New Jersey and Delmarva barrier islands. In: Davis RA Jr (ed) Geology of Holocene barrier island systems. Springer, Berlin, pp 207–232

Oost AP, de Boer PL (1994) Sedimentology and development of barrier islands, ebb-tidal deltas, inlets and backbarrier areas of the Dutch Wadden Sea. In: Flemming BW, Hertweck G (eds) Tidal flats and barrier systems of continental Europe: a selected overview. Senckenberg marit 24:65–115

Owen MW (1971) The effect of turbulence on the settling velocities of silt flocs. In: 14th congress of the international association of hydraulic research, Paris, Proceedings, pp 27–32

Park YA, Davis RA Jr (eds) (2001) Proceedings of Tidalites 2000. Special publication, Korean Society of Oceanography, Seoul, 103 pp

Pejrup M (1988) The triangular diagram used for classification of estuarine sediments: a new approach. In: de Boer PL, van Gelder A, Nio SD (eds) Tide-influenced sedimentary environments and facies. D Reidel Publishing Company, Dordrecht, pp 289–300

Pejrup M, Andersen TJ (2000) The influence of ice on sediment transport, deposition and reworking in a temperate mudflat area, the Danish Wadden Sea. Cont Shelf Res 20:1621–1634

Pestrong R (1972) Tidal-flat sedmentation at Colley Landing, southwest San Francisco Bay. Sed Geol 8:251–288

Pilkey OH (2003) A celebration of the world's barrier islands. Columbia University Press, New York

Pilkey OH, Neal WJ, Monteiro JH, Dias JMA (1989) Algarve barriers islands: a noncoastal-plain system in Portugal. J Coast Res 5:239–261

Postma H (1961) Transport and accumulation of suspended matter in the Dutch Wadden Sea. Neth J Sea Res 1:148–190

Postma H (1982) Hydrography of the Wadden Sea: movements and properties of water and particulate matter. In: Wadden Sea Working Group (eds) Final report on 'hydrography'. AA Balkema, Rotterdam

Pratt BR, James NP, Cowan CA (1992) Peritidal carbonates. In: Walker RG, James NP (eds) Facies models – response to sea level change, 2nd edn. Geological Association of Canada, pp 303–322

Reimnitz E (1966) Late Quaternary history and sedimentation of the Copper River Delta and vicinity, Alaska. Ph.D. thesis, University of California, San Diego

Reineck H-E (1958) Longitudinale Schrägschichtung im Watt. Geol Rundschau 37:73–82

Reineck H-E (1960) Über Zeitlücken in rezenten Flachseesedimenten. Geol Rundschau 49:149–161

Reineck H-E (1976) Drift ice action on tidal flats, North Sea. Rev Geogr Montr 30:197–200

Reineck H-E (1987) Morphologische Entwicklung der Insel Mellum. In: Gerdes G, Krumbein WE, Reineck H-E (eds) Mellum – Portrait einer Insel. Kramer, Frankfurt, pp 87–99

Reineck H-E, Singh IB (1980) Depositional sedimentary environments, 2nd edn. Springer, Berlin

Reineck H-E, Wunderlich F (1968) Classification and origin of flaser and lenticular bedding. Sedimentology 11:99–104

Ridderinkhof H (1988) Tidal and residual flows in the western Dutch Wadden Sea: I. Numerical model results. Neth J Sea Res 22:1–26

Rinaldo A, Belluco E, D'Alpeos A, Feola A, Lanzoni S, Marani A (2004) Tidal networks: form and function. In: Fagherazzi S, Marani A, Blum LK (eds) The ecogeomorphology of tidal marshes. American Geophysical Union, Washington, DC, pp 75–91

Roy PS, Cowell PJ, Ferland MA, Thom BG (1994) Wave-dominated coasts. In: Carter RWG, Woodroffe CD (eds) Coastal evolution: Late Quaternary shoreline evolution. Cambridge University Press, Cambridge, pp 121–185

Schäfer W (1972) Ecology and palaeoecology of marine environments. Oliver & Boyd, Edinburgh, 538 pp

Schieber J (2004) Microbial mats in the siliciclastic rock record. In: Eriksson PK, Altermannn DR, Nelson DR, Mueller WE, Catuneanu O (eds) The Precambrian earth: tempos and events. Elsevier, Amsterdam, pp 663–673

Schieber J, Southard JB (2009) Bedload transport of mud by floccules ripples – Direct observation of ripple migration processes and their implications. Geology 37:483–486

Schneider JF (1975) Recent tidal deposits, Abu Dhabi, UAE, Arabian Gulf. In: Ginsburg RN (ed) Tidal deposits. Springer, New York, pp 209–214

Schneider-Storz B, Nebelsick JH, Wehrmann A, Federolf C (2008) Comparative taphonomy of three bivalves from mass shell accumulation in the macrotidal regime of North Sea tidal flats. Facies 54:461–478

Schwartz ML (ed) (1973) Barrier islands. Benchmark papers in geology 9. Dowden, Hutchinson & Ross, Stroudsburg

Shepard FP (1954) Nomenclature based on sand-silt-clay ratios. J Sed Petrol 24:151–158

Smith DG, Reinson GE, Zaitlin BA, Rahmani RA (eds) (1991) Clastic tidal sedimentology. Can Soc Petrol Geol Mem 16

Speer PE, Aubrey DG (1985) A study of non-linear tidal propagation in shallow inlet/estuarine systems, Part II: Theory. Estuar Coast Shelf Sci 21:207–224

Stanev EV, Flemming BW, Bartholomä A, Staneva JV, Wolff J-O (2007) Vertical circulation in shallow tidal inlets and back-barrier basins. Cont Shelf Res 27:798–831

Stanev EV, Grayek S, Staneva J (2009) Temporal and spatial circulation patterns in the East Frisian Wadden Sea. Ocean Dyn 59:167–181

Streif HJ (1990) Das ostfriesische Küstengebiet – Nordsee, Inseln, Watten und Marschen. Sammlung geologischer Führer 57. Gebr Borntraeger, Berlin

Terwindt JHJ (1988) Palaeo-tidal reconstructions of inshore tidal depositional environments. In: de Boer PL, van Gelder A, Nio SD (eds) Tide-influenced sedimentary environments and facies. D Reidel Publishing Company, Dordrecht, pp 233–263

Thomas RG, Smith DG, Wood JM, Visser J, Calverley-Range EA, Koster EH (1987) Inclined heterolithic stratification – terminology, description, interpretation and significance. Sed Geol 53:123–179

van der Spek AJF (1995) Reconstruction of tidal inlet and channel dimensions in the Frisian Middelzee, a former tidal basin in the Dutch Wadden Sea. In: Flemming BW, Bartholomä A (eds) Tidal signatures in modern and ancient sediments. Int Assoc Sediment Spec Publ 24:239–258

van der Spek AJF (1996) Holocene depositional sequences in the Dutch Wadden Sea south of Ameland. In: Beets DJ, Fischer MM, de Gans W (eds) Coastal studies on the Holocene of the Netherlands. Mededel Rijks Geol Dienst 57:41–69

van der Wegen M, Roelvink JA (2008) Long-term morphodynamic evolution of a tidal embayment using a two-dimensional, process-based model. J Geophys Res C03016. doi:10.1029/2006JC003983

van der Wegen M, Dastgheib A, Roelvink JA (2010) Morphodynamic modeling of tidal channel evolution in comparison to empirical PA relationship. Coastal Eng 57:827–837

van Dongeren AR, de Vriend HJ (1994) A model of morphological behaviour of tidal basins. Coastal Eng 22:287–310

van Ledden M, van Kesteren WGM, Winterwerp JC (2004) A conceptual framework for the erosion behaviour of sand-mud mixtures. Cont Shelf Res 24:1–11

van Straaten LMJU (1952) Biogene textures and the formation of shell beds in the Dutch Wadden Sea. Koninkl Ned Akad Wetenschap, Amsterdam, Ser B 55:500–516

van Straaten LMJU (1954) Composition and structure of recent marine sediments in the Netherlands. Leidse Geol Mededel 19:1–110

van Straaten LMJU (1964) De bodem der Waddenzee. In: Anderson WF, Abrahamse J, Buwalda JD, van Straaten LMJU (eds) Het Waddenboek. Nederl geol Vereeniging, pp 75–151

van Straaten LMJU, Kuenen PH (1957) Accumulation of fine-grained sediments in the Wadden Sea. Geol Mijn 19:329–354

van Straaten LMJU, Kuenen PH (1958) Tidal action as a cause of clay accumulation. J Sed Petrol 28:406–413

van Veen J (1950) Eb- en vloedschaar systemen in de Nederlandse getijwateren. Tijdschrift van het Koninklijk Nederlandsch Aardrijkskundig Genootschap, Tweede Reeks LXVII:303–325

Visser MJ (1980) Neap-spring cycles reflected in Holocene subtidal large-scale bedform deposits: a preliminary note. Geology 8:543–546

Vos PC, van Kesteren WP (2000) The long-term evolution of intertidal mudflats in the northern Netherlands during the Holocene; natural and anthropogenic processes. Cont Shelf Res 20:1687–1710

Walther F (1972) Zusammenhänge zwischen der Größe der Ostfriesischen Seegaten mit ihren Wattgebieten sowie den Gezeiten und Strömungen. Jahrber Forschungstelle Norderney 23:7–32

Walton TL Jr, Adams WD (1976) Capacity of inlet outer bars to store sand. In: Proceedings, 15th international conference on coastal engineering. ASCE, Honolulu, Hawaii, pp 1919–1937

Warrick AW (2002) Soil physics companion. CRC Press, Boca Raton, 389 pp

Williams E (1960) Intra-stratal flow and convolute folding. Geol Mag 97:208–214

Williams PB, Orr MK, Garrity NJ (2002) Hydraulic geometry: a geomorphic design tool for tidal marsh channel evolution in wetland restoration projects. Restoration Ecol 10:577–590

Wunderlich F (1967) Die Entstehung von "convolute bedding" an Platenrändern. Senckenberg lethaea 48:345–349

Xu W (2000) Mass physical sediment properties and trends in a Wadden Sea tidalbasin. Berichte, Fachbereich Geowissenschaften, Universität Bremen, No. 157